

Application of ANFIS to the design of elliptical CFST columns

Ngoc-Long Tran, Trong-Cuong Vo, Duy-Duan Nguyen, Van-Quang Nguyen,
Huy-Khanh Dang and Viet-Linh Tran*

Department of Civil Engineering, Vinh University, Vinh 461010, Vietnam

(Received May 18, 2021, Revised April 26, 2023, Accepted April 27, 2023)

Abstract. Elliptical concrete-filled steel tubular (CFST) column is widely used in modern structures for both aesthetical appeal and structural performance benefits. The ultimate axial load is a critical factor for designing the elliptical CFST short columns. However, there are complications of geometric and material interactions, which make a difficulty in determining a simple model for predicting the ultimate axial load of elliptical CFST short columns. This study aims to propose an efficient adaptive neuro-fuzzy inference system (ANFIS) model for predicting the ultimate axial load of elliptical CFST short columns. In the proposed method, the ANFIS model is used to establish a relationship between the ultimate axial load and geometric and material properties of elliptical CFST short columns. Accordingly, a total of 188 experimental and simulation datasets of elliptical CFST short columns are used to develop the ANFIS models. The performance of the proposed ANFIS model is compared with that of existing design formulas. The results show that the proposed ANFIS model is more accurate than existing empirical and theoretical formulas. Finally, an explicit formula and a Graphical User Interface (GUI) tool are developed to apply the proposed ANFIS model for practical use.

Keywords: adaptive neuro-fuzzy inference system; elliptical concrete-filled steel tubular short column; explicit formula; graphical user interface; ultimate axial load

1. Introduction

Nowadays, the concrete-filled steel tubular (CFST) members have become increasingly used in engineering constructions because of their structural benefits (i.e., high strength, high ductility and energy absorption, and excellent fire and seismic resistance) (Espinosa *et al.* 2011, Yang *et al.* 2008). Besides, the external steel tubular of CFST columns is used as formwork during the construction phase, thus leading to speed up the construction process and reducing costs (Moon *et al.* 2012). Furthermore, through the interaction between the steel tubular and the concrete core, the local buckling of the steel tubular is delayed by the restraint of the concrete, and the concrete strength is increased by the confining effect of the steel tubular.

Recently, elliptical CFST columns have been favored by architects and engineers worldwide as key structural elements for high-rise buildings, airport terminals, or bridges. An elliptical CFST column is known as a new composite column type of CFST family. It is made by filling concrete into elliptical hollow steel tubular, as shown in Fig. 1. In this figure, the symbols P , L , D , B , and t indicate the axial compression load, the length of the column, the major axis diameter, the minor

*Corresponding author, Ph.D., E-mail: vietlinh.dhv@gmail.com

axis diameter, and the thickness of the steel tubular, respectively. Owing to its reasonable distribution of the major-minor axis, elliptical CFST columns also reveal a better architectural aesthetics appearance and a small fluid resistance coefficient (Chan *et al.* 2010).

Currently, the existing design code for composite construction, such as AS5100 (2004), AISC (2016), ACI (2014), and Eurocode 4 (EC-4) (2011) do not provide a methodology for the design of elliptical CFST columns. Therefore, many researchers recommended using the rules established for circular or rectangular CFST columns for designing the elliptical CFST columns. Nevertheless, this alternative usage seems not very appropriate since the structural behaviors of rectangular and circular CFST columns are not the same as those of elliptical CFST columns.

Obviously, the most reliable method to accurately evaluate the behavior of elliptical CFST short columns is the experimental study on actual structures. In the last two decades, a number of experimental studies and theoretical models have been developed to investigate the behaviors of elliptical CFST short columns. Notably, Zhao and Packer (2009) carried out a test with 13 experimental specimens of elliptical CFST short columns. Both normal concrete and self-consolidating concrete were used in this testing program. The load-carrying capacity of these elliptical CFST short columns was compared with that predicted by design codes. Based on the experimental data, the authors proposed a design formula to calculate the ultimate axial load of elliptical CFST short columns. The results obtained from this proposed formula were agreed with that from the test. Liu and Zha (2011) conducted a test with 6 elliptical CFST short columns under axial load and proposed a formula for predicting the ultimate axial load of elliptical CFST short columns. The comparative study showed that this formula can accurately calculate the ultimate axial load compared with the test results. Jamaluddin *et al.* (2013) reported the results of 26 elliptical CFST short columns subjected to axial compressive load. Based on the EC4 provisions (2011), they suggested a new equation for predicting the capacities of elliptical CFST short columns. Generally, the predicted results were very close to those measured from the experiments.

Because of being time-consuming and expensive, usually experiments are not always possible to perform. Therefore, finite element (FE) analysis, which takes into account the nonlinear behaviors of materials, is beneficial. Shen *et al.* (2015) developed a FE model of elliptical CFST short columns under axial compressive loading using ABAQUS software. This FE model was validated by comparing it against test results. Then, a simplified formula was proposed to estimate the ultimate axial load of elliptical CFST short columns. Dai and Lam (2010a) conducted a FE analysis to examine the performance of elliptical CFST short columns. The FE model was verified by using the experimental test results of Yang *et al.* (2008). Patel *et al.* (2016) performed numerical simulation using both FE and fiber element techniques to simulate the concrete confining pressure in short circular, elliptical and octagonal CFST columns. The results showed that both ultimate axial strengths and complete axial load-strain curves obtained from the FE model and fiber element model agreed reasonably well with experimental results. Liu *et al.* (2017) used the FE simulation to obtain the inelastic behaviors of elliptical CFST short columns. However, they did not consider the nonlinear strain hardening of the hot-rolled steel in their FE model. Furthermore, the FE models have been used to investigate the performance of elliptical CFST short columns by Sheehan *et al.* (2012), Hassanein *et al.* (2018), Ahmed *et al.* (2021). Evidently, the FE results could successfully capture the experimental observations. Therefore, it can be adopted to enlarge the database by conducting the parametric study.

Nowadays, machine learning (ML) is known as a powerful approach that is capable of coping with complex input-output problems (Cai *et al.* 2020, Cook *et al.* 2019, Dauji, 2020, Luat *et al.* 2020, Vahidi *et al.* 2017, Xue and Zhou 2018, Yaylacı *et al.* 2020). ML models are particularly

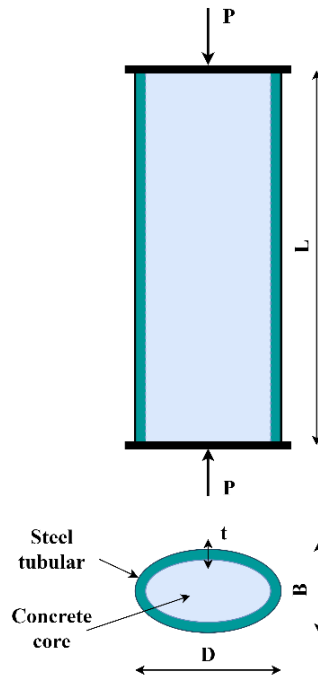


Fig. 1 Elliptical CFST column under axial compression load

useful in engineering applications where classical approaches failed, or they are too complicated to be applied (Duan *et al.* 2021, Nguyen *et al.* 2022, Sadrmomtazi *et al.* 2013, Tran and Kim 2023a, b). For this reason, many research studies have been carried out to estimate the structural capacity of CFST columns using the ML approaches (Asteris *et al.* 2021, Ly *et al.* 2021, Sarir *et al.* 2021, Tran *et al.* 2023). Ahmadi *et al.* (2014, 2017) used an artificial neural network (ANN) to predict the axial capacity of short CFST columns. Moon *et al.* (2014) have successfully developed a fuzzy logic model for predicting the strength of circular CFST short columns. Guneyisi and Ipek (2016, 2019) derived a gene expression programming model to predict the load-bearing capacity of circular CFST columns. Naderloo *et al.* (2012) developed an adaptive neurofuzzy inference system (ANFIS) model to predict crop yield based on different energy inputs. The results showed that the ANFIS model could predict the grain yield with good accuracy. Keshavarzi *et al.* (2017) compared the ANFIS-based subtractive clustering algorithm with different input combinations as well as sequential regression models for simulation of variations in soil cation exchange capacity. The obtained results showed that the ANFIS model had the ability to estimate soil CEC by computing easily measurable variables with a guarantee of authenticity, reliability, and reproducibility. Umrao *et al.* (2018) proposed a predictive ANFIS model for estimation of unconfined compressive strength (UCS) and modulus of elasticity (E) of sedimentary rocks. The high accuracy in predicting the UCS and E of sedimentary rocks indicated that the proposed ANFIS model can be confidently used in the field of geotechnical engineering. Ren *et al.* (2019) employed support vector machine and particle swarm optimization to determine the axial capacity of square CFST columns. Tran *et al.* (2019a, b) developed a neural network-based model to predict the axial compression capacity of circular and square CFST columns. In addition, the explicit formulas were derived based on the ANN models for practical application. Tran *et al.* (2020) compared three

Table 1 Existing formulas for ultimate axial load prediction of elliptical CFST short columns

Author	Formula (s)	Eq.
Zhao and Packer (2009)	$P_{Zhao} = \eta_s A_s f_y + [1 + \eta_c (t/D_e) (f_y/f_c')] A_c f_c'$ $D_e = 2a \{1 + [1 - 2.3(t/2a)^{0.6}] (a/b) - 1\},$ $\eta_s = 0.25(3 + 2\lambda),$ $\eta_c = 4.9 - 18.5\lambda + 17\lambda^2,$ $\lambda = \sqrt{\frac{A_s f_y + 0.85 A_c f_c'}{(\pi^2 EI)/(\mu L)^2}},$ $EI = E_s I_s + E_c I_c,$	(1)
Liu and Zha (2011)	$P_{Liu} = f_{sc} (A_s + A_c),$ $f_{sc} = \frac{1 + 1.5(b/a)^{0.3} \xi}{1 + A_s/A_c} f_{ck},$ $\xi = (A_s f_y)/(A_c f_{ck}),$ $f_{ck} = 0.67 f_{cu},$	(2)
Jamaluddin et al. (2013)	$P_{Jamaluddin} = \eta_s A_s f_y + [1 + \eta_c (t/D_e) (f_y/f_c')] A_c f_c'$ $D_e = 2a^2/b,$ $\eta_s = 0.25(3 + 2\lambda),$ $\eta_c = 4.9 - 18.5\lambda + 17\lambda^2,$ $\lambda = \sqrt{\frac{A_s f_y + 0.85 A_c f_c'}{(\pi^2 EI)/(\mu L)^2}},$ $EI = E_s I_s + 0.6 E_c I_c,$	(3)
Shen (2015)	$P_{Shen} = f_{sc} (A_s + A_c),$ $f_{sc} = (A + B\xi + C\xi^2 + D\xi^3) f_{ck},$ $\xi = (A_s f_y)/(A_c f_{ck}),$ $f_{ck} = 0.67 f_{cu},$ $A = 1.3625$ $B = 0.7080$ $C = 0.0624$ $D = 0.0075$	(4)
Ahmed and Liang (2020)	$P_{Ahmed} = A_s f_y + A_c (\gamma_c f_c' + 4.1 f_{rp,Ahmed}),$ $f_{rp,Ahmed} = \begin{cases} 1.065\xi + 3.449 & \text{for } 1.5 \leq a/b < 2 \\ 1.019\xi + 0.304 & \text{for } a/b \geq 2 \end{cases}$ $\xi = (A_s f_y)/(A_c \gamma_c f_c'),$ $\gamma_c = 1.85 D_c^{-0.135} \quad (0.85 \ll \gamma_c \ll 1)$	(5)

advanced data-driven models for predicting the axial compression capacity of CFST columns. The comparative results showed that three data-driven models achieved more accuracy than existing equations. Generally, the performance of such ML-based models has been shown to be better than the existing formulas found in the literature. However, most ML-based studies so far have concentrated on the columns with a circular and rectangular cross-section. Therefore, more investigations are required to assess the potential applications of ML-based models for studying the axial behavior of elliptical CFST short columns.

This study aims to develop an efficient ANFIS for predicting the ultimate axial load of elliptical CFST columns. ANFIS is a hybrid intelligent system that combines the learning power of ANN

with the knowledge representation of fuzzy logic (Jang 1993). Therefore, ANFIS can handle the limitations of both ANN and fuzzy logic methods and offers an excellent opportunity to solve difficult and complex problems (Armaghani and Asteris 2021, Tran and Kim 2020). Although the datasets observed from the tests at the laboratory are valuable, it is not practical to collect such datasets for all potential scenarios. Therefore, numerical simulation of elliptical CFST short columns subjected to pure axial compression is performed using ABAQUS software in this study. The validity of the FE model was examined by comparing with test results in the literature. Consequently, 92 experimental datasets selected from the literature and 96 numerical FE datasets of elliptical CFST short columns are used to develop the ANFIS models. As a result, a total of 63 ANFIS models are developed and the best one is chosen based on the performance indices. The accuracy of the proposed ANFIS model is compared with the results of the existing formulas. Finally, new explicit formulas and a Graphical User Interface (GUI) tool are developed to apply the proposed ANFIS model for practical use.

2. Research significance

In the design of elliptical CFST columns, the ultimate axial load is one of the most critical parameters. However, there are still challenges to developing a generalized analytical formula for accurately predicting the ultimate axial load of elliptical CFST columns. Design codes for composite construction, such as AS51006 (2004), AISC (2016), ACI (2014), and EC-4 (2011), do not provide a method for designing elliptical CFST columns. Moreover, conducting experiments is not always possible because of being time-consuming and expensive. Therefore, it is necessary to develop an efficient ML model and a practical tool for estimating the ultimate axial load of elliptical CFST columns.

To fill these gaps, this study develops an efficient ANFIS model to improve the ultimate axial load prediction of elliptical CFST columns using the collected experimental data from the literature and numerical simulation results generated in this study. In addition, explicit formulas and a GUI tool developed in this study can rapidly predict the ultimate axial load with less effort. They can provide initial estimates of outcomes before performing extensive laboratory or fieldwork.

3. Existing formulas

A brief review of existing formulas for calculating the ultimate axial load of elliptical CFST columns is presented in this section. Zhao and Packer (2009) conducted an experimental program to investigate the behavior of elliptical CFST columns. The tests included both normal concrete and self-consolidating concrete. Moreover, different loading methods, such as loading through steel alone, loading through concrete alone, and loading through the whole cross-section were investigated. Based on the experimental results, a formula was proposed to predict the load-carrying capacity of elliptical CFST columns. According to Liu and Zha (2011), the plastic equilibrium theory was used to determine the distribution rule for the interaction force between the steel tube and the core concrete in elliptical CFST columns under axial load, and finite element simulation was used to determine the lateral stress of the core concrete. Then the effectively confined zone distribution of core concrete was assumed to account for the two results above.

Based on the idea of “unified theory” and the existing unified formulas for circular CFST stub columns, the author proposed a new unified equation for elliptical CFST columns. Jamaluddin *et al.* (2013) carried out twenty-six specimens of elliptical CFST columns to investigate the axial compressive behavior. In addition, the study developed a new equation based on the EC-4 provision (2011) for predicting the ultimate axial load of elliptical CFST columns. Based on the data fitting of numerical simulation results and the idea of "unified theory" as Liu and Zha study (2011), Shen (2015) proposed another formula to calculate the ultimate axial load of elliptical CFST columns. Shen (2015) used the same formula to predict the ultimate uniaxial compressive strength of the elliptical CFST columns as that of Liu and Zha (2011), but it is different in calculating the unified strength (f_{sc}). Recently, Ahmed and Liang (2020), proposed a new confinement model for determining the lateral stresses on the filled concrete in the elliptical CFST columns. It was included in the computational fiber-based model for the nonlinear simulation of elliptical CFST short columns under axial load. The experimental results were used to validate the accuracy of the computer simulation method. It has been shown that the developed confinement model for elliptical CFST columns yields more accurate results than those which were modified for circular CFST columns. Moreover, the fiber-based model has been demonstrated to be a computationally efficient and accurate simulation technology for elliptical CFST columns. Besides, a design equation was given to determine the ultimate axial load of elliptical CFST short columns. The results showed that this equation outperformed design codes and previous studies. The detailed expressions of the formulas developed by Zhao and Packer (2009), Liu and Zha (2011), Jamaluddin *et al.* (2013), Shen (2015), and Ahmed and Liang (2020) are summarized in Table 1.

4. Numerical modelling

In this section, a FE model is developed to simulate the behavior of elliptical CFST short columns using ABAQUS software (2014). The FE model was validated against the experimental results (Jamaluddin *et al.* 2013, Yang *et al.* 2008) by comparing ultimate axial loads and axial load-axial strain behavior.

4.1 Material models

4.1.1 Model of elliptical steel tubular

The idealized stress-strain model proposed by Liang (2009) is used to simulate the elastic-plastic behavior of steel elliptical tubular, which is shown in Fig. 2. In this figure, ε represents the axial strain in steel elements, σ indicates the longitudinal stress at the strain ε , f_y indicates the strength of steel at the yield point, ε_y is the yield strain at the strength f_y , and ε_t is taken as 0.005 for structural steel and $10\varepsilon_y$ for high strength steel. The ultimate strain (ε_u) is taken as 0.1 and 0.2 for structural and high strength steels, respectively. Young's modulus (E_s) and Poisson's ratio (ν) of the steel were chosen as 200,000 N/mm^2 and 0.3, respectively.

In the FE model, the engineering stress-strain curve of steel was converted to true stress-true plastic strain curve by using Eqs. (6) and (7):

$$\sigma_{true} = \sigma_{norm}(1 + \varepsilon_{norm}) \quad (6)$$

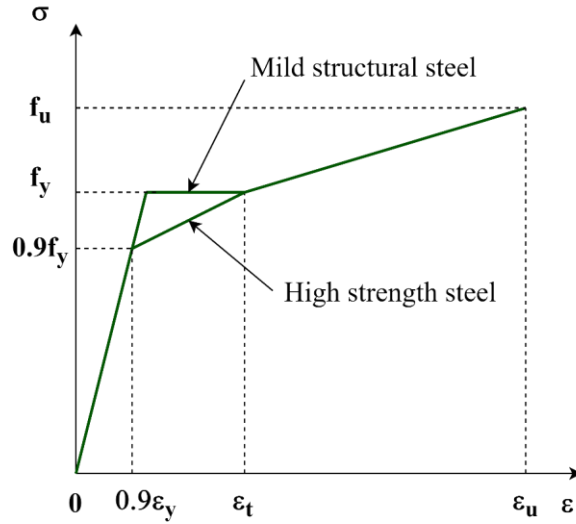


Fig. 2 Idealised stress-strain curves for steels

$$\varepsilon_{true} = \ln(1 + \varepsilon_{norm}) \quad (7)$$

where σ_{norm} and ε_{norm} are the nominal engineering stress and nominal engineering strain, respectively, σ_{true} and ε_{true} are the true stress and true strain, respectively.

4.1.2 Model of confined concrete core

The idealised model of the confined concrete core is illustrated in Fig. 3. In this model, the stress-strain response is characterised into three parts. The first part (i.e., OA) is expressed as follows (Mander *et al.* 1988, Patel *et al.* 2016):

$$\sigma_c = \frac{f'_{cc} \lambda \left(\frac{\varepsilon_c}{\varepsilon'_{cc}} \right)}{\lambda - 1 + \left(\frac{\varepsilon_c}{\varepsilon'_{cc}} \right)^\lambda} \quad (8)$$

The second and third parts can be expressed as (Patel *et al.* 2016):

$$\sigma_c = \begin{cases} f'_{cc} + \frac{(f_e - f'_{cc})(\varepsilon_c - \varepsilon'_{cc})}{\varepsilon_e - \varepsilon'_{cc}} & \text{for } \varepsilon'_{cc} < \varepsilon_c \ll \varepsilon_e \\ f_e + \frac{(f_{cu} - f_e)(\varepsilon_c - \varepsilon_e)}{\varepsilon_{cu} - \varepsilon_e} & \text{for } \varepsilon_e < \varepsilon_c \ll \varepsilon_{cu} \end{cases} \quad (9)$$

The related parameters of Eqs. (8) and (9) are calculated as follows (Mander *et al.* 1988, Patel *et al.* 2016):

$$\lambda = \frac{E_c}{E_c - \left(\frac{f'_{cc}}{\varepsilon'_{cc}} \right)} \quad (10)$$

$$E_c = 3320 \sqrt{f'_{cc}} + 6900 \text{ (MPa)} \quad (11)$$

$$\varepsilon'_c = \begin{cases} 0.002 & \text{for } \gamma_c f'_c \ll 28 \text{ (MPa)} \\ 0.002 + \frac{\gamma_c f'_c - 28}{54000} & \text{for } 28 < \gamma_c f'_c \ll 82 \text{ (MPa)} \\ 0.003 & \text{for } \gamma_c f'_c > 82 \text{ (MPa)} \end{cases} \quad (12)$$

$$f'_{cc} = \gamma_c f'_c + k_1 f_{rp} \quad (13)$$

$$\varepsilon'_{cc} = \varepsilon'_c \left(1 + k_2 \frac{f_{rp}}{\gamma_c f'_c} \right) \quad (14)$$

$$\gamma_c = 1.85 D_c^{-0.135} \quad (0.85 \ll \gamma_c \ll 1) \quad (15)$$

$$k_1 = 6.7 - 2.6 \left(\frac{a}{b} \right) \quad (16)$$

$$k_2 = 20.5 \quad (17)$$

$$f_{rp} = \left(0.037 - 0.00755 \frac{(a+b)}{t} \right) f_y \quad (17 \ll \frac{a+b}{t} \ll 29) \quad (18)$$

$$f_e = \alpha_c f'_{cc} \quad (19)$$

$$f_{cu} = \beta_c f'_{cc} \quad (20)$$

$$\alpha_c = 0.889 - 0.004 \gamma_c f'_c \quad (21)$$

$$\beta_c = 0.841429 - 0.005714 \gamma_c f'_c \quad (22)$$

where σ_c illustrates the longitudinal stress in concrete element, ε_c indicates the concrete axial strain, f'_{cc} denotes the ultimate strength of confined concrete, ε'_{cc} represents the axial strain at f'_{cc} , ε'_c is the axial strain at f'_c , and f'_c is the ultimate strength of unconfined concrete, D_c is the concrete core diameter along the major axis which is determined as $2(a-t)$, t represents the steel tube thickness, a is the major axis radius of elliptical section, b denotes the minor axis radius, f_{rp} illustrates the confining pressure applied by steel tubular on the concrete core, $\varepsilon_e = 10\varepsilon'_c$ and $\varepsilon_{cu} = 30\varepsilon'_c$ denote the concrete strains at points B and C, respectively.

The Drucker-Prager formulation was employed in the concrete material. The angle of friction, flow-stress ratio and dilation angle were chosen respectively as 20° , 0.8 and 0.001 based on the sensitivity study given by Patel *et al.* (2016).

4.2 Element types, boundary conditions, and interaction contact

Although both solid and shell element type could be appropriate to simulate the deformation and local buckling features of the steel tubular. However, the large shell thickness could obviously influence the ability of the mesh in the steel tubular to follow the curved contact boundary. This will significantly affect the accuracy of FE model on the concrete confinement effect and interaction between the concrete core and the steel tubular. Using solid element not only made the steel tubular meshes follow the curved contacting boundary reasonably, but also expressed the

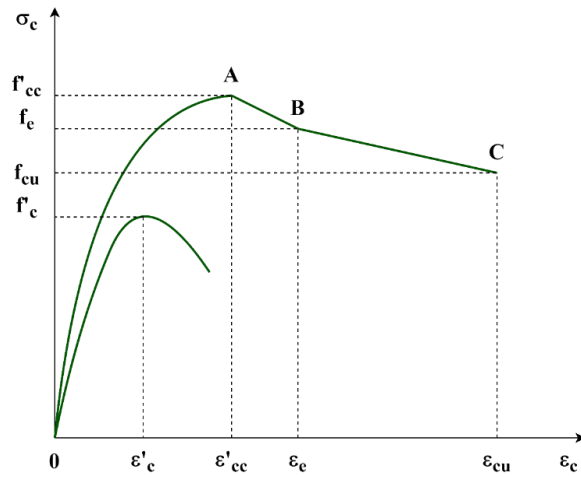


Fig. 3 Idealised stress-strain relation of confined concrete

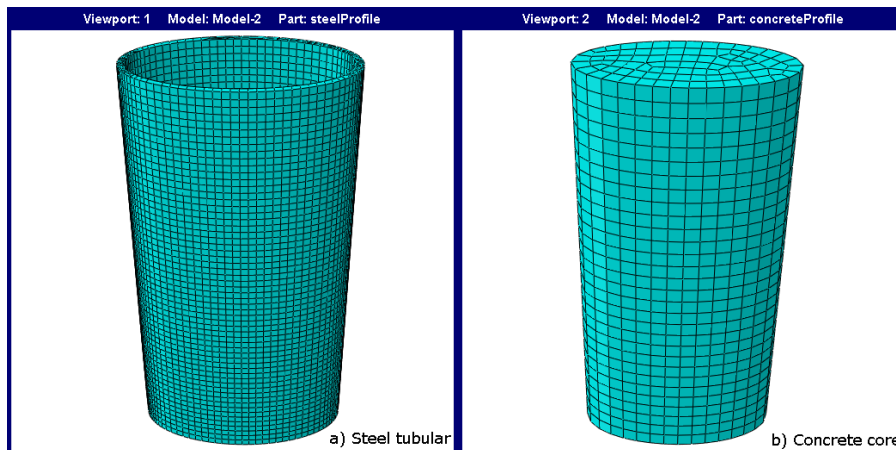


Fig. 4 Mesh of FE model

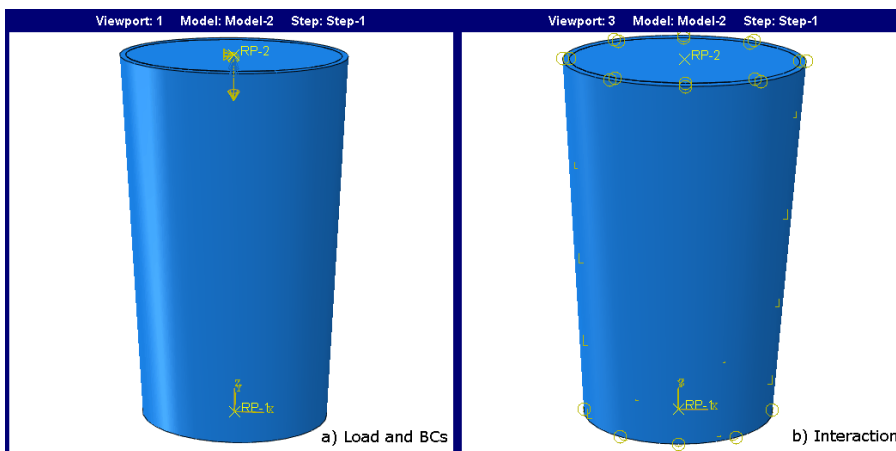


Fig. 5 Boundary condition and interaction contact of FE model

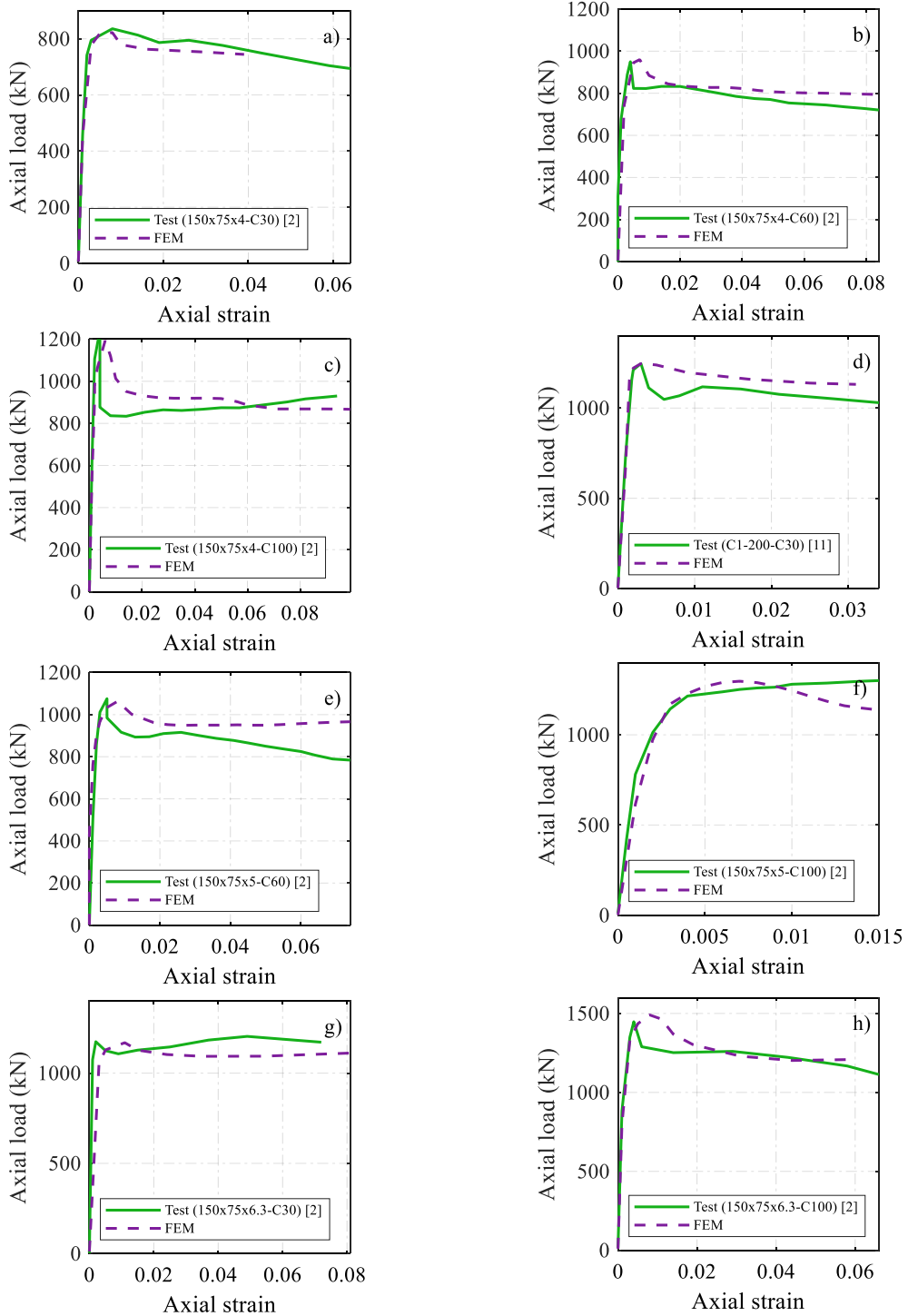


Fig. 6 Comparison of axial load-strain responses between FE results and experimental results (Yang *et al.* 2008)

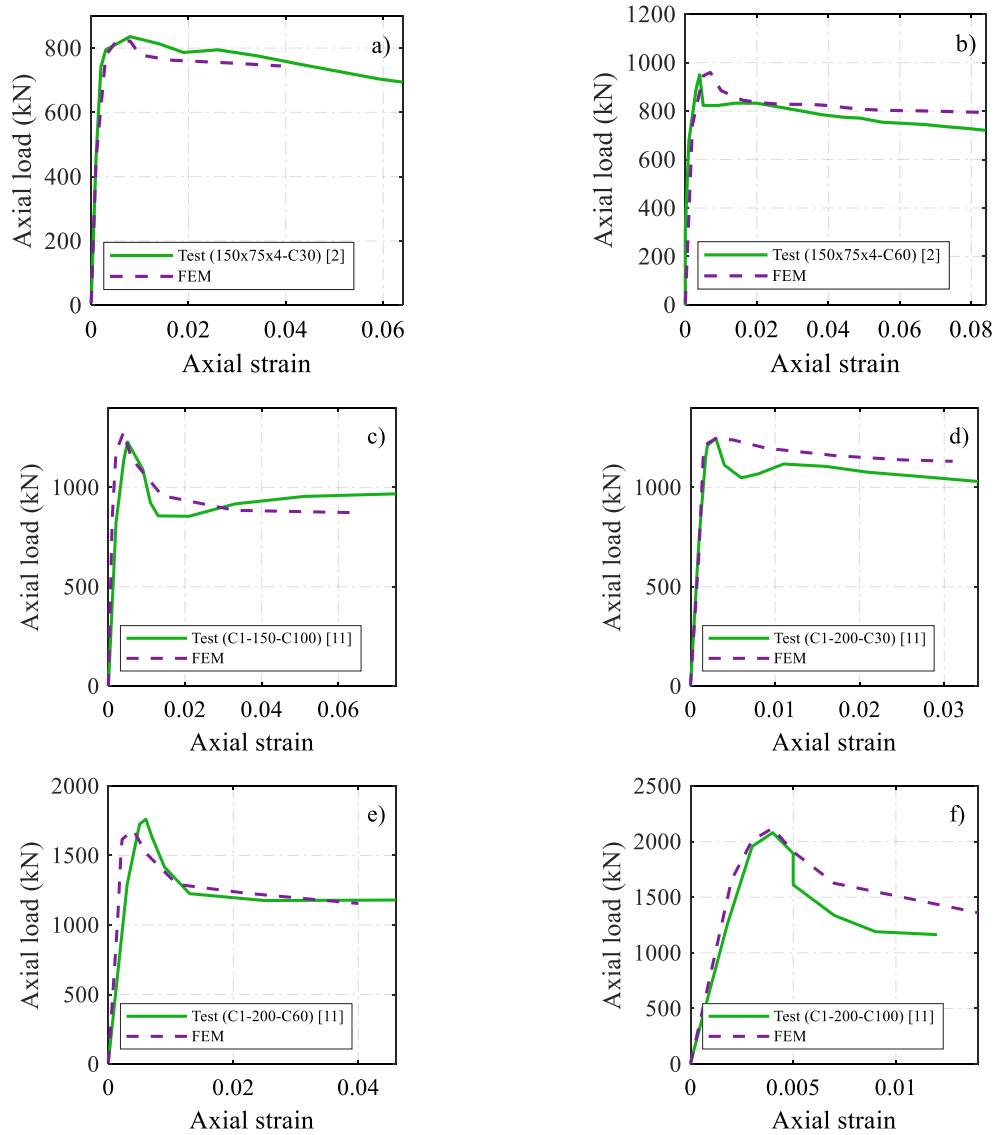


Fig. 7 Comparison of axial load-strain responses between FE results and experimental results (Jamaluddin *et al.* 2013)

deformation along the thickness direction of the steel tubular. For this reason, both elliptical steel tubular and concrete core are modelled with 8-node solid element C3D8R in this study. According to Dai and Lam (2010b), the mesh sizes of steel tubular with 5-10 mm and concrete with 10-20 mm should be used. In addition, the concrete element sizes should be about two times the element sizes of the steel tubular. Therefore, the element mesh size of 5 mm for the steel tubular and 10 mm for the concrete core are used in the FE model in this study, as shown in Fig. 4.

The 'Surface-to-Surface' option is used to define the contact action between the steel tubular and the concrete core. The penalty function with a friction coefficient of 0.3 is applied to define the tangential contact, which offered a better coincidence compared to the experiments (Dai and

Table 2 Comparison of ultimate axial load between FE results and experimental results

Specimen	L	D	B	t	f_y	f'_c	$P_{u,exp}$	$P_{u,FEM}$	$\frac{P_{u,FEM}}{P_{u,exp}}$
	(mm)	(mm)	(mm)	(mm)	(MPa)	(MPa)	(kN)	(kN)	
150x75x4-C30	300.00	150.40	75.60	4.18	376.50	26.93	839.00	835.09	0.995
150x75x4-C60	300.00	150.57	75.52	4.19	376.50	47.30	974.00	983.86	1.010
150x75x4-C100	300.00	150.39	75.67	4.18	376.50	84.57	1265.00	1206.98	0.954
150x75x5-C30	300.00	150.12	75.65	5.12	369.00	26.93	981.00	942.58	0.961
150x75x5-C60	300.00	150.23	75.74	5.08	369.00	47.30	1084.00	1063.35	0.981
150x75x5-C100	300.00	150.28	75.67	5.09	369.00	84.57	1296.00	1295.99	1.000
150x75x6.3-C30	300.00	148.78	75.45	6.32	400.50	26.93	1193.00	1168.77	0.980
150x75x6.3-C100	300.00	149.53	75.35	6.25	400.50	84.57	1483.00	1530.80	1.032
CI-150-C30	300.00	150.10	75.00	4.10	431.40	35.80	900.00	929.58	1.033
CI-150-C60	301.00	150.20	75.10	4.00	431.40	49.43	1139.00	1173.60	1.030
CI-150-C100	299.00	150.10	75.20	4.20	431.40	92.14	1239.00	1278.46	1.032
CI-200-C30	398.00	197.80	100.10	5.10	347.90	36.87	1232.00	1246.29	1.012
CI-200-C60	398.00	197.50	100.20	5.10	347.90	53.54	1737.00	1683.10	0.969
CI-200-C100	398.00	197.40	100.10	5.10	347.90	102.26	2116.00	2120.39	1.002
Mean									0.99
StD									0.03
CoV									0.03

Table 3 Statistical properties of the database

	L	D	B	t	f_y	f'_c	P_u
	(mm)	(mm)	(mm)	(mm)	(MPa)	(MPa)	(kN)
Minimum	160.00	85.40	57.00	1.00	201.00	25.00	389.10
Mean	344.27	173.85	89.41	4.98	378.21	67.03	1594.20
Maximum	698.00	318.50	155.00	9.72	612.00	102.26	3334.09
Standard deviation	101.04	37.44	18.51	2.04	62.67	25.51	745.63
Coefficient of variation	0.29	0.22	0.21	0.41	0.17	0.38	0.47

Lam 2010b). The normal contact is set as ‘Hard Contact’. For the columns, the top and bottom ends of the steel tubular and concrete core are fixed against all degrees of freedom except the axial displacement at the loaded end. Both the boundary and the load conditions are imposed to the reference point (RP) which is coupled to the lower and upper surface of the column. A specified axial displacement is applied to the reference node at the loading point. The general static analysis step is adopted. The boundary condition and interaction contact of the FE model is depicted in Fig. 5.

4.3 Analysis procedure

To provide an initial imperfection mode shape, a linear eigenvalue analysis is firstly conducted

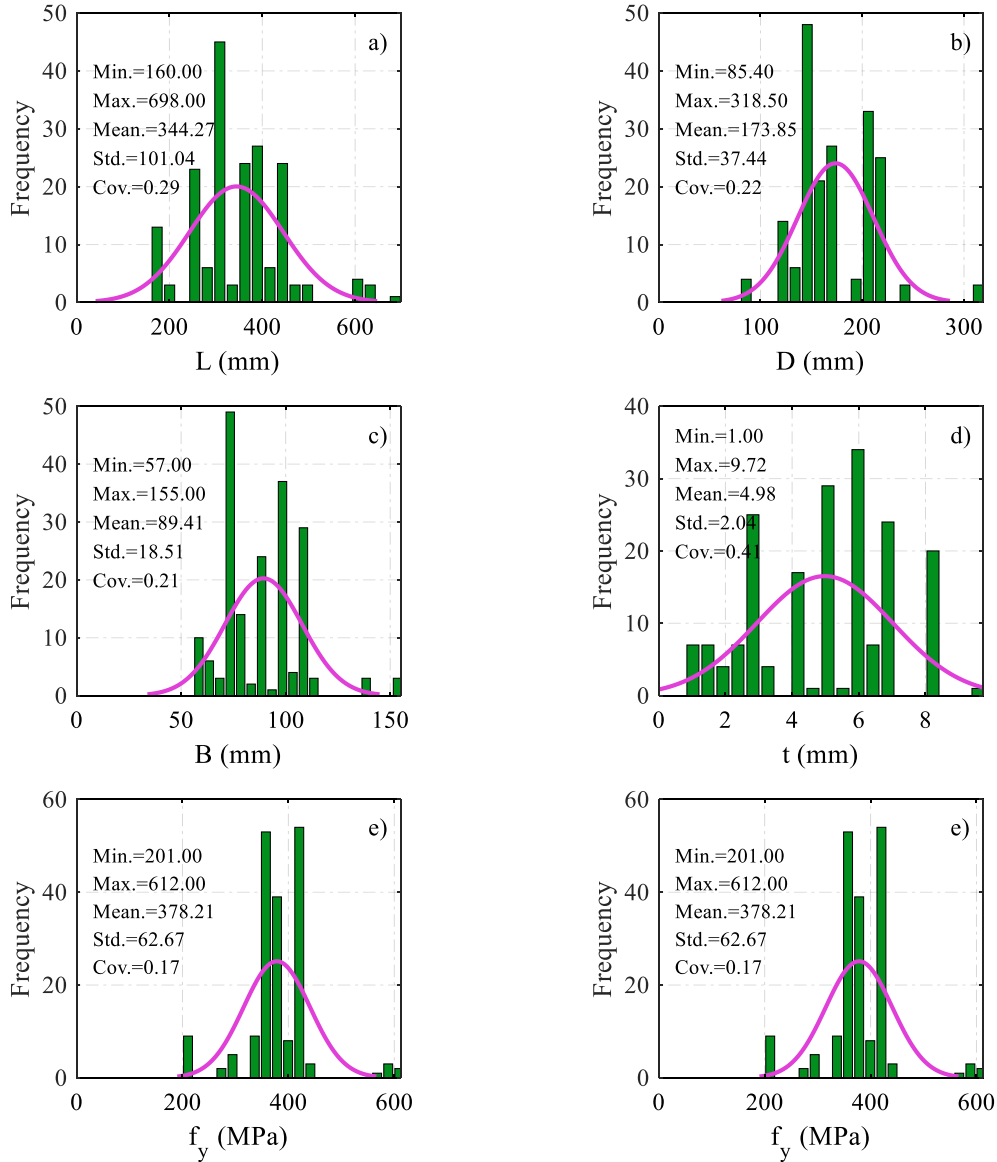


Fig. 8 Distribution of data information

for each column model. The global buckling mode with the lowest eigenvalue is selected as the initial imperfect geometry. The initial geometrical imperfection is taken as the lowest buckling mode shape with an amplitude of $t_s/100$ (Chan and Gardner 2008), where t_s is the wall thickness of the steel tubular. For the parametric study, this imperfection amplitude is used throughout. In the second step, the displacement-controlled static analysis is performed to simulate the nonlinear behavior of elliptical CFST short columns. Note that the residual stresses are not considered in the FE model.

4.4 Verification of the FE model

The verification of the FE model is presented against the tests conducted by Yang *et al.* (2008) and Jamaluddin *et al.* (2013). Fig. 6 and 7 show the comparison of the axial load versus axial strain curves of the experimental and FE results. Additionally, the comparisons of ultimate axial load between the experimental and FE results are given in Table 2. The results show that the FE model developed in this study could provide a feasible and reliable prediction for the ultimate axial load of elliptical CFST short columns.

5. Database

In this study, 92 experimental datasets of elliptical CFST short columns are collected from the tests conducted by Yang *et al.* (2008), Zhao and Packer (2009), Dai and Lam (2010b), Lam *et al.* (2010), Jamaluddin *et al.* (2013), Uenaka (2014), Chan *et al.* (2015), and Yang *et al.* (2017). In this database, only the elliptical section specimens under monotonic uniaxial compression are selected and six geometric and material properties were included, such as the length of the column (L), the major axis diameter (D), the minor axis diameter (B), the thickness of the steel tubular (t), the yield strength of the steel tubular (f_y), and the compressive strength of concrete (f_c').

Additionally, based on the validated FE model developed in Section 3, extensive datasets of elliptical CFST short columns are generated. Herein, three elliptical steel tubular types are chosen to keep the $(a + b)/t$ ratios within the limits of the f_{rp} stress in the range of 17 to 29 as suggested by Patel *et al.* (2016). Four concrete compressive strengths of 70, 80, 90, and 100 MPa were considered with two steel grades of 355 and 420 MPa. The column lengths were fixed to three times the greater width (D) of the cross-section to avoid the overall instability effects as well as end conditions. As a result, 96 FE datasets are generated in this study. Finally, the database that combined the experimental and FE datasets are used to develop the ANFIS model. It can be seen that the database involves a wide variety of the yield strength of steel and compressive strength of concrete for both normal-strength and high-strength concrete in the range from 201.00 to 612.00 MPa and 25.0 to 102.26 MPa, respectively. The column length is varied from 160.00 to 636.00 mm. The major axis diameter is ranged between 85.40 mm and 318.50 mm. The minor axis diameter is varied from 57.00 to 155.00 mm. The thickness of the steel tubular is changed from 1.00 to 8.00 mm. In this study, the concrete compression strength of the cylinder specimen is used. Nevertheless, it is found out that some experimental studies only showed the cube specimens for the compressive strength of the concrete. For this reason, the cube concrete compressive strength was approximately converted equally to the concrete cylinder compressive strength by means of the conversion factors suggested by Ding *et al.* (2011). In summary, the range and statistical properties of the database are shown in Table 3 and Fig. 8.

6. Adaptive neuro-fuzzy inference system

6.1 Basic structure

The adaptive neuro-fuzzy inference system (ANFIS) is a hybrid intelligent system, which merges the recognition and adaptability capacity of ANN with the ability of the decision-making capacity of the fuzzy logic system. ANFIS has been introduced in detail by many studies (Kar *et*

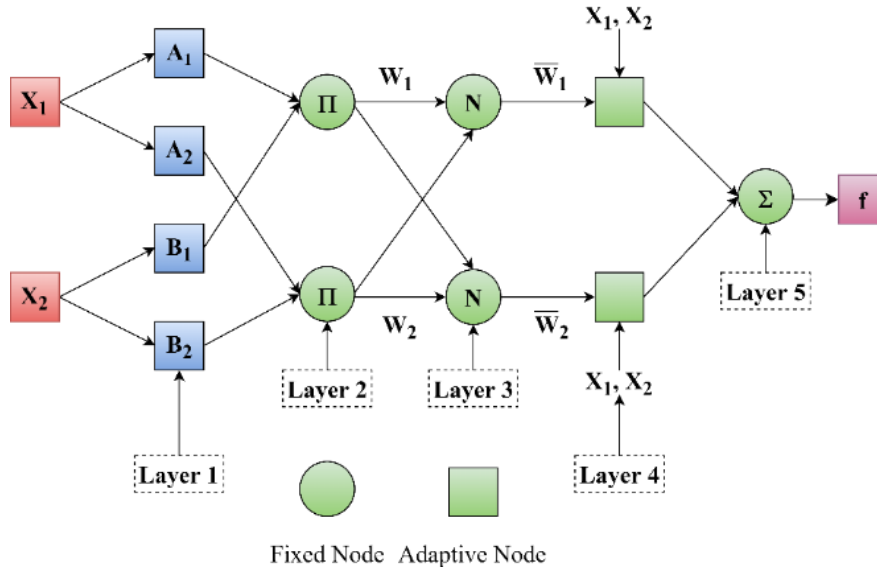


Fig. 9 Basic structure of ANFIS model

Table 4 ANFIS rules

Number	Rule
Rule 1	If X_1 is $C1_{X1}$ and X_2 is $C1_{X2}$ and X_3 is $C1_{X3}$ and X_4 is $C1_{X4}$ and X_5 is $C1_{X5}$ and X_6 is $C1_{X6}$ the Y is CL_1 ,
Rule 2	If X_1 is $C2_{X1}$ and X_2 is $C2_{X2}$ and X_3 is $C2_{X3}$ and X_4 is $C2_{X4}$ and X_5 is $C2_{X5}$ and X_6 is $C2_{X6}$ the Y is CL_2 ,
Rule 3	If X_1 is $C3_{X1}$ and X_2 is $C3_{X2}$ and X_3 is $C3_{X3}$ and X_4 is $C3_{X4}$ and X_5 is $C3_{X5}$ and X_6 is $C3_{X6}$ the Y is CL_3 ,
Rule 4	If X_1 is $C4_{X1}$ and X_2 is $C4_{X2}$ and X_3 is $C4_{X3}$ and X_4 is $C4_{X4}$ and X_5 is $C4_{X5}$ and X_6 is $C4_{X6}$ the Y is CL_4 ,
Rule 5	If X_1 is $C5_{X1}$ and X_2 is $C5_{X2}$ and X_3 is $C5_{X3}$ and X_4 is $C5_{X4}$ and X_5 is $C5_{X5}$ and X_6 is $C5_{X6}$ the Y is CL_5 ,
Rule 6	If X_1 is $C6_{X1}$ and X_2 is $C6_{X2}$ and X_3 is $C6_{X3}$ and X_4 is $C6_{X4}$ and X_5 is $C6_{X5}$ and X_6 is $C6_{X6}$ the Y is CL_6

al. 2020, Kar and Biswal 2020, Shariati *et al.* 2020). The basic structure of ANFIS can be seen in Fig. 9.

As shown in this figure, the first layer gets the inputs, normalizes, and converts them into fuzzy values. This layer has parameters that control the position of each fuzzy set. The outputs of the first layer are the prior values of the membership function (MF) in accordance with the input of the fuzzy system. In the second layer, the MFs normalize the MFs' weights between 0 and 1. The third layer captures the rule base of the fuzzy inference system (FIS). The fourth layer then generates the outputs values of the MFs' weights. Finally, the fifth layer obtains the output values of the whole model. In order to explain the architecture of the FIS, assuming the system has two inputs, X_1 and X_2 , and an output, f , two fuzzy *If – then* rules for the first-degree Sugeno fuzzy model, which are expressed in Eqs. (23) and (24).

Table 5 Gaussian membership function's parameters

MFs	Parameters	Inputs					
		X_1^N	X_2^N	X_3^N	X_4^N	X_5^N	X_6^N
C1	σ	0.126	0.084	0.048	0.128	0.160	0.208
	c	0.097	0.296	0.223	0.087	0.183	0.047
C2	σ	0.085	0.079	0.119	0.075	0.057	0.177
	c	0.491	0.525	0.085	0.673	0.451	0.708
C3	σ	0.091	0.060	0.057	0.108	0.072	0.152
	c	0.286	0.302	0.210	0.448	0.444	0.791
C4	σ	0.050	0.029	0.108	0.131	0.091	0.165
	c	0.265	0.302	0.213	0.375	0.494	0.237
C5	σ	0.068	0.073	0.097	0.067	0.021	0.114
	c	0.363	0.385	0.322	0.529	0.447	0.637
C6	σ	0.094	0.082	0.084	0.071	0.076	0.182
	c	0.503	0.551	0.516	0.663	0.499	0.803

Table 6 Weights of the rules

Number	Weight's relationship
W_{Rule1}	$(C1_{X1}) \times (C1_{X2}) \times (C1_{X3}) \times (C1_{X4}) \times (C1_{X5}) \times (C1_{X6})$
W_{Rule2}	$(C2_{X1}) \times (C2_{X2}) \times (C2_{X3}) \times (C2_{X4}) \times (C2_{X5}) \times (C2_{X6})$
W_{Rule3}	$(C3_{X1}) \times (C3_{X2}) \times (C3_{X3}) \times (C3_{X4}) \times (C3_{X5}) \times (C3_{X6})$
W_{Rule4}	$(C4_{X1}) \times (C4_{X2}) \times (C4_{X3}) \times (C4_{X4}) \times (C4_{X5}) \times (C4_{X6})$
W_{Rule5}	$(C5_{X1}) \times (C5_{X2}) \times (C5_{X3}) \times (C5_{X4}) \times (C5_{X5}) \times (C5_{X6})$
W_{Rule6}	$(C6_{X1}) \times (C6_{X2}) \times (C6_{X3}) \times (C6_{X4}) \times (C6_{X5}) \times (C6_{X6})$

$$\text{Rule 1: If } X_1 \text{ is } A_1 \text{ and } X_2 \text{ is } B_1, \text{ then } f_1 = m_1X_1 + n_1X_2 + q_1, \quad (23)$$

$$\text{Rule 2: If } X_1 \text{ is } A_2 \text{ and } X_2 \text{ is } B_2, \text{ then } f_2 = m_2X_1 + n_2X_2 + q_2, \quad (24)$$

where A_1 , A_2 , B_1 , and B_2 are the MFs for inputs X_1 and X_2 , respectively, and m_1 , n_1 , q_1 , m_2 , n_2 , and q_2 are the parameters of the output function.

6.2 Sub-clustering approach

Clustering is a task of assigning the datasets into groups called clusters to discover structures and patterns in the datasets. The radius of a cluster is the maximum distance between all the points and the centroid. Sub-clustering is based on classifying each point of the dataset just to one cluster. This method assumes that each data point is a potential cluster center and calculates the potential for each data point based on the density of surrounding data points (Mirrashid 2014). The data points with the highest remaining potential as the next cluster center and the potential of data points near the new cluster center are destroyed. It is notable that the influential radius of the cluster is critical for determining the number of clusters and data points outside this radius. Also, a

smaller radius leads to many smaller clusters in the data space, which results in more rules (Chiu, 1994). Mamdani (1975) and Sugeno (1985) are two main types of the FIS. Because the Sugeno system is more compact and efficient than a Mamdani system, it was used in this study. For more detailed descriptions, the reader can also refer to the work in Refs. (Kar *et al.* 2020, Sun *et al.* 2020, Vakhshouri and Nejadi 2018).

7. Performance indices

To evaluate the performances of predicted models, three statistical indices, including the coefficient of determination (R^2), the root mean squared error ($RMSE$) and $a20 - index$, are used, which are expressed as follows

$$R^2 = 1 - \left(\frac{\sum_{i=1}^n (t_i - o_i)^2}{\sum_{i=1}^n o_i^2} \right), \quad (25)$$

$$RMSE = \sqrt{\left(\frac{1}{n} \right) \sum_{i=1}^n (t_i - o_i)^2}, \quad (26)$$

$$a20 - index = \frac{m20}{M}, \quad (27)$$

where t_i and o_i are the target and predicted value of i^{th} sample, respectively, n is the number of samples, and $m20$ is the summation of samples with the ratio of the predicted value to a target value falling between 0.80 and 1.20 (Armaghani *et al.* 2019, Asteris and Mokos 2020).

8. ANFIS model for ultimate axial load of elliptical CFST short columns

8.1 Input and output variables

In order to develop the ANFIS model, the length of the column (L), the major axis diameter (D), the minor axis diameter (B), the thickness of the steel tubular (t), the yield strength of the steel tubular (f_y), and the compressive strength of concrete (f_c') were considered as input variables. The output variable was the ultimate axial load of the elliptical CFST short column (P_u). In order to enhance the accuracy of the ANFIS model and to avoid unexpected errors during the training process, the database were normalized within the range of 0 and 1. Accordingly, normalization was implemented by dividing each value of input and output variables by the corresponding minimum and maximum, which are expressed as follows

$$X_i^N = \frac{(X - X_{min})}{(X_{max} - X_{min})}, \quad (28)$$

where X is the data sample, X_i^N is the normalized data sample, X_{min} and X_{max} are the minimum and maximum values of considered parameters, respectively.

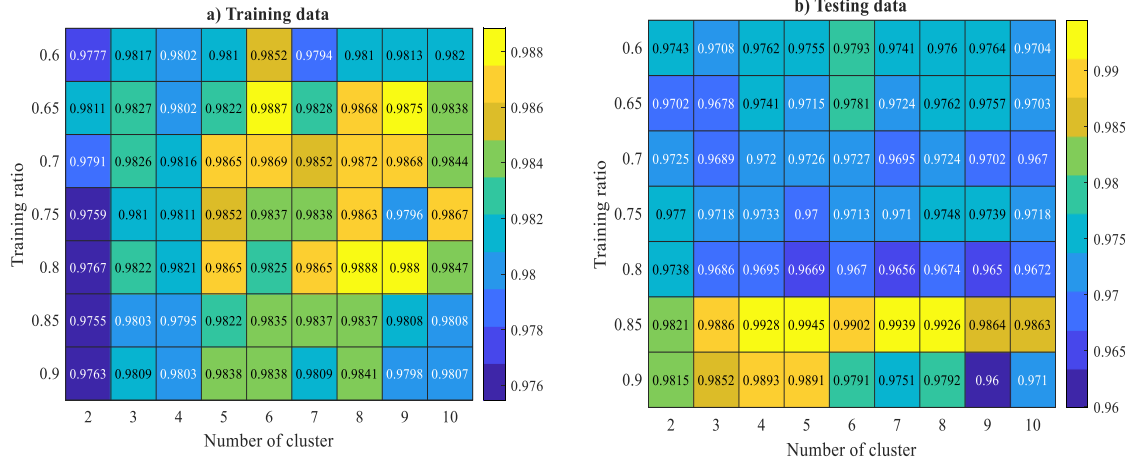


Fig. 10 R^2 value of diferent ANFIS models

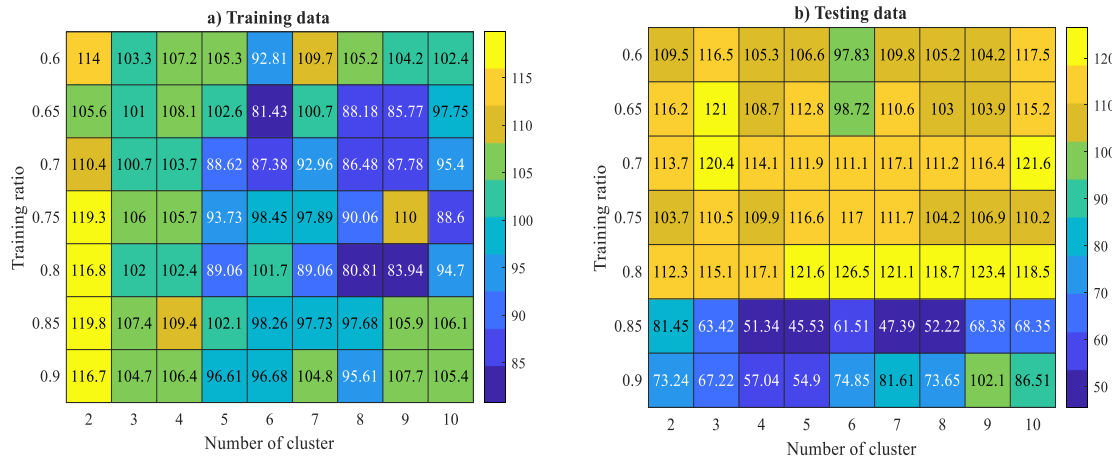


Fig. 11 $RMSE$ value in kN of diferent ANFIS models

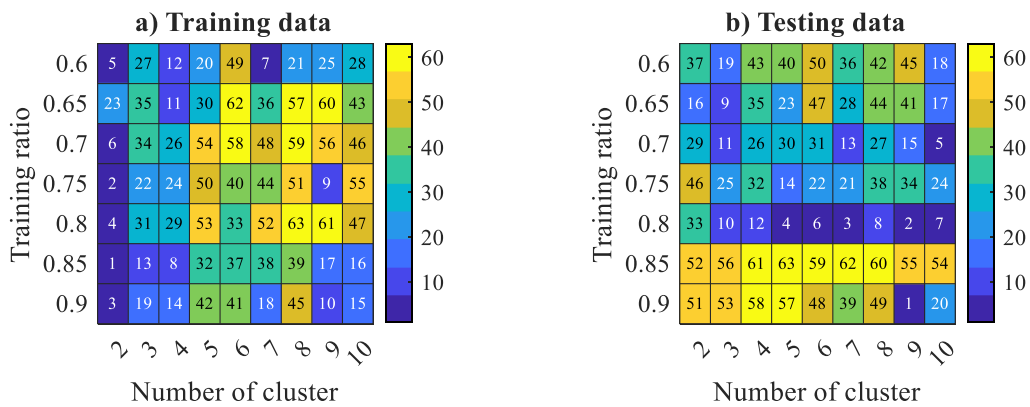


Fig. 12 Ranking of R^2

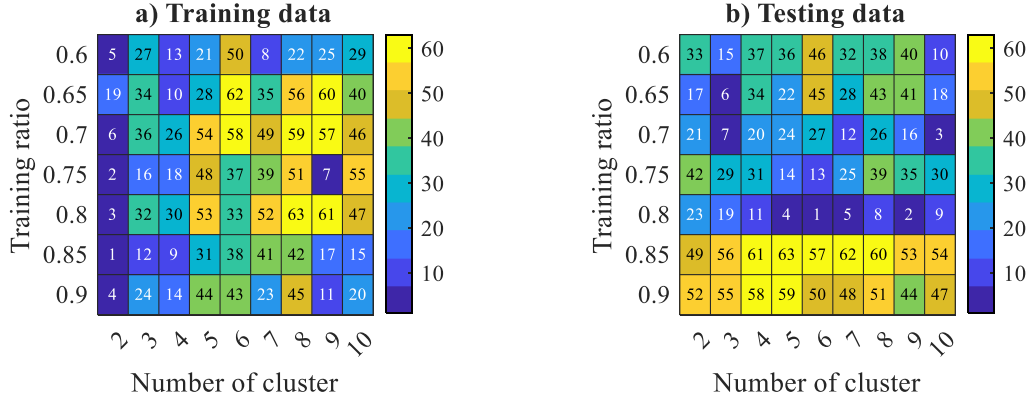


Fig. 13 Ranking of *RMSE*

8.2 Membership function

Membership function (MF) has an inevitable effect on the established neuro-fuzzy model to predict the comparable values with the implemented outputs. It defines how each point in the input space is mapped to a membership value between 0 and 1. In this study, Gaussian MF was found as a proper one for the proposed ANFIS model. It has the advantage of being smooth and non-zero at all points, which is expressed in Eq. (29).

$$\mu(x, \sigma, c) = e^{-\frac{(x-c)^2}{2\sigma^2}}, \tag{29}$$

where σ is the variance and c is the mean of x .

8.3 Number of clusters

The clusters in the ANFIS model are expressed as the linear functions, which are given in Eq. (30).

$$CL_i = a_{i1}X_1^N + a_{i2}X_2^N + a_{i3}X_3^N + a_{i4}X_4^N + a_{i5}X_5^N + a_{i6}X_6^N + C_i, \quad i = 1, \dots, n. \tag{30}$$

where the parameters a_{i1} to a_{i6} and C_i are coefficients of X_1^N to X_6^N , corresponding to cluster i^{th} .

To determine the number of clusters for ANFIS model, the database was randomly split and shuffled into 7 groups of training and testing ratio and the number cluster varied from 2 to 10. Each model was trained first by using the training datasets and then testing datasets were applied to evaluate the performance of each model. A total of 63 ANFIS models are developed in this study.

The performance of these models based on the R^2 and *RMSE* indices are shown in Figs. 10-14. Generally, all 63 ANFIS models perform well on the current database. To determine the best ANFIS model, the ranking method proposed by Zorlu *et al.* (2008) was applied using two performance indices (i.e., R^2 and *RMSE*), as shown in Figs. 10-11. Accordingly, the developed models (63 models) were sorted from 1 to 63 based on their performances. Herein, the value of 1 denotes the lowest performance, and 63 means the highest performance of the model. In this way,

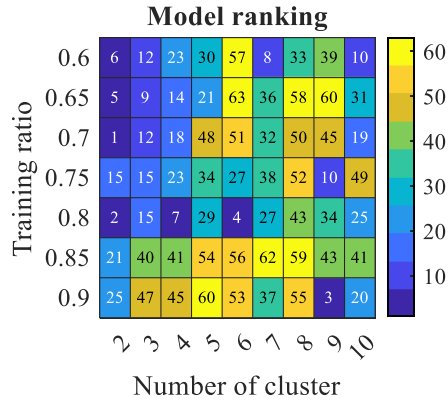


Fig. 14 Total model ranking

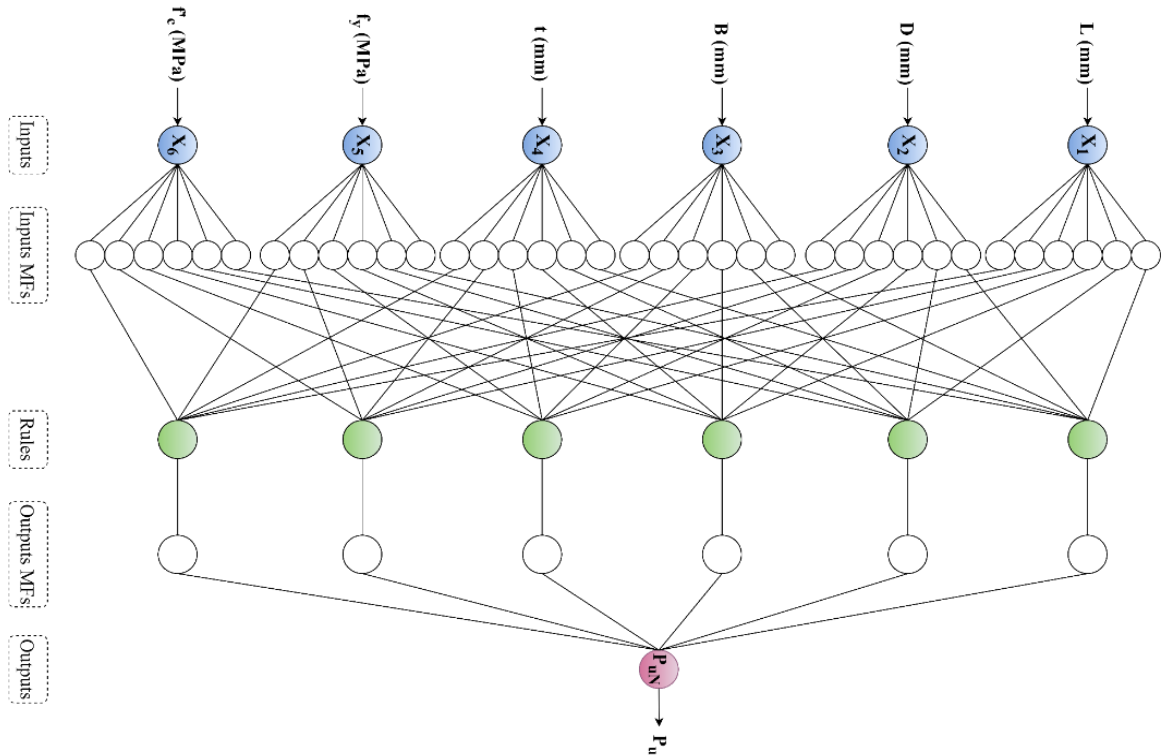


Fig. 15 Proposed ANFIS structure

each performance index was ranked separately and merged as a total ranking for model evaluation, as shown in Figs. 12 and 13. Fig. 14 shows that the ANFIS model with 0.7 of training ratio combined with 2 clusters provides the worst performance, meanwhile, the ANFIS model with 0.65 of training ratio combined with 6 clusters obtains the best performance in predicting the ultimate axial load of elliptical CFST short columns with 0.9887 and 0.9781 of R^2 and 81.43 kN and 98.72 of $RMSE$ for training and testing datasets, respectively.

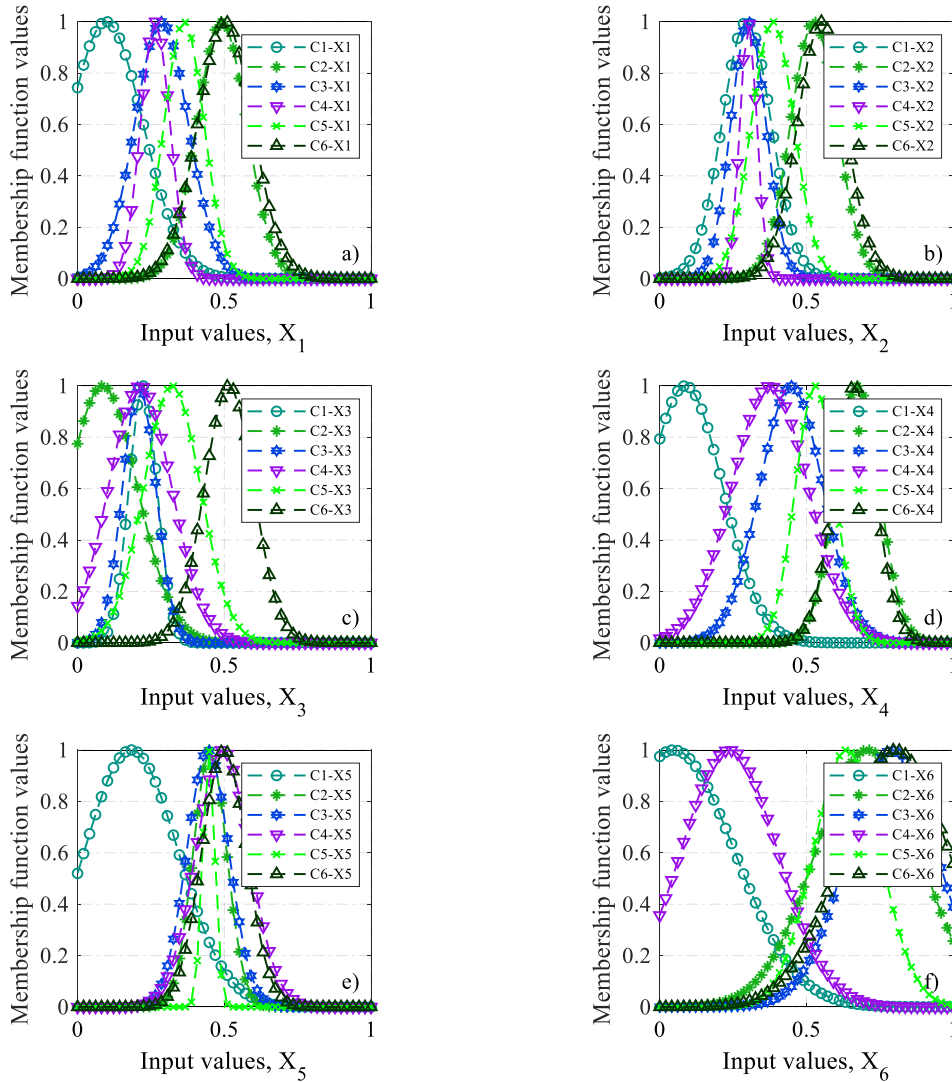


Fig. 16 Membership functions for input variables

The structure of the best ANFIS model is shown in Fig. 15. It is noted that the colored circle indicates a fixed node and the white circle implies an adaptive node. In this model, six Gaussian MFs and six linear MFs are used for input and output variables, respectively, and six fuzzy rules have been constructed during the training process. The ANFIS rules, Gaussian MFs parameters and the weights of the rules are presented in Tables 4-6. Additionally, MFs of all the inputs of the proposed ANFIS model are plotted in Fig. 16.

8.4 Performance of the proposed ANFIS model

Fig. 17 shows the prediction performance in a regression form for the training, testing and all datasets of the proposed ANFIS model. As shown in this figure, the *RMSE* of the training,

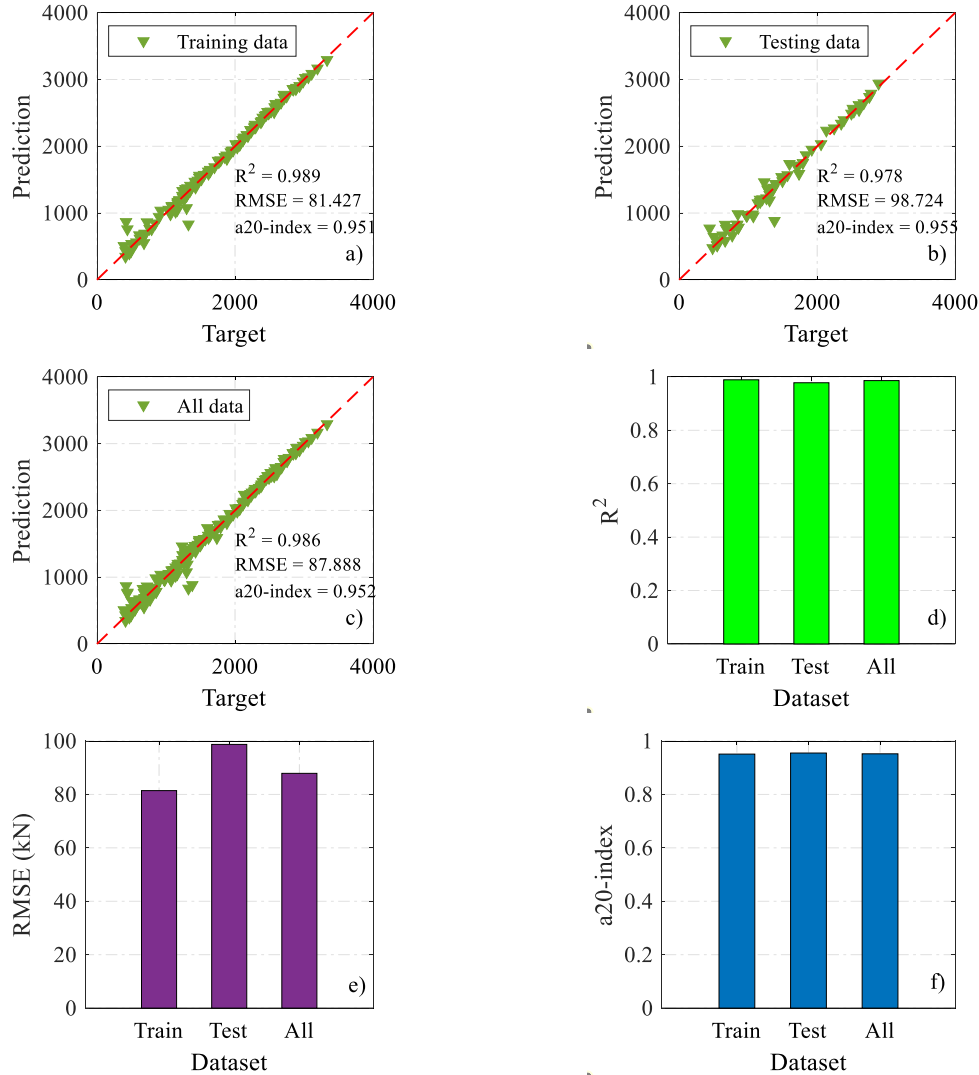


Fig. 17 Performance of the proposed ANFIS model

testing, and all datasets are 81.427, 98.724, and 87.888, respectively. Evidently, the $RMSE$ value is quite low compared to the ultimate axial load range of 389.10 to 3334.09 kN. Additionally, the values of R^2 for training, testing and all datasets are found to be 0.989, 0.978, and 0.986, respectively. The overall response with R^2 close to 1 verifies that the proposed ANFIS model has acceptable performance for estimating the ultimate axial load of elliptical CFST short columns.

9. Comparison of the proposed ANFIS model with existing formulas

In order to compare the results of the proposed ANFIS model with existing formulas, three performance indices of R^2 , $RMSE$ and $a20 - index$ were used. The comparative results are

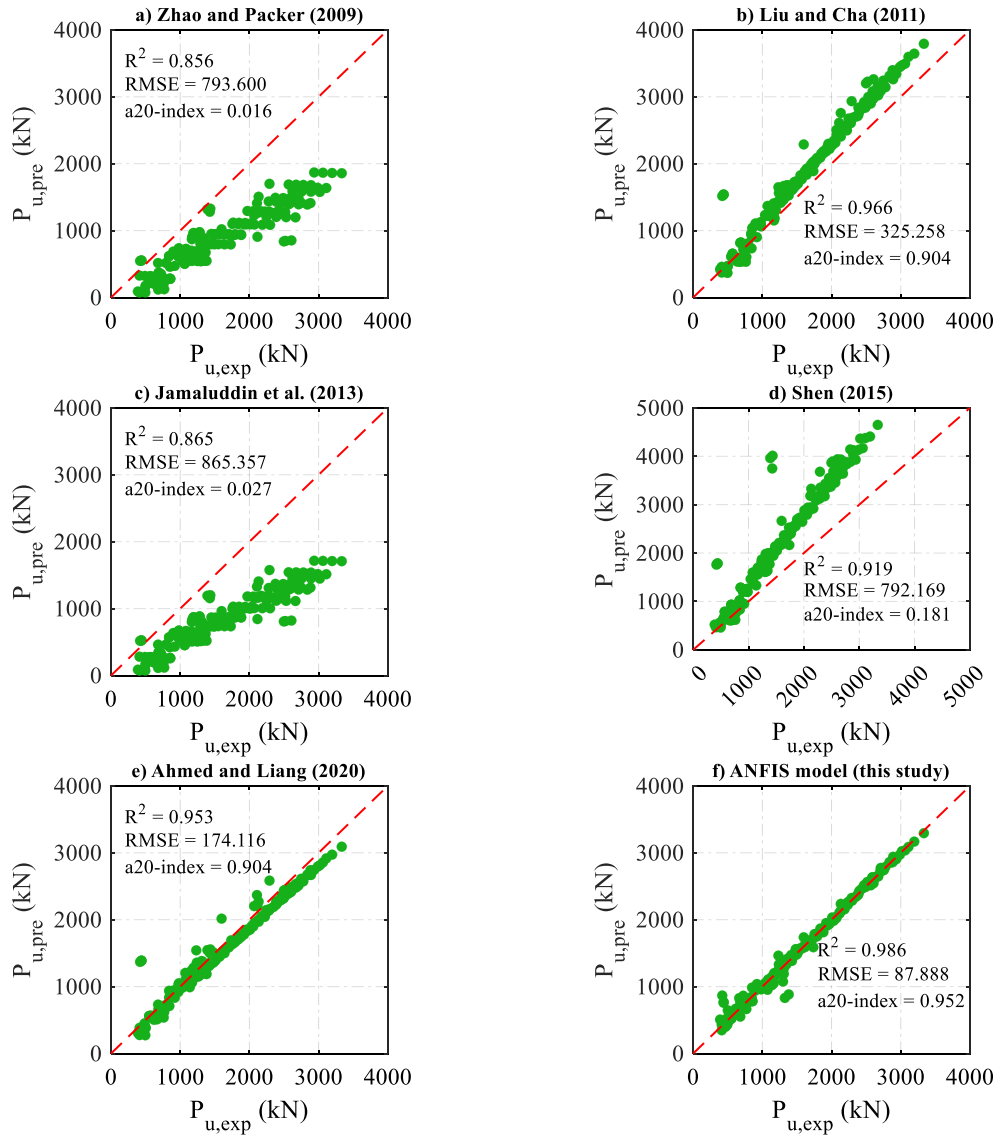


Fig. 18 Comparison between the proposed ANFIS model and the existing formulas

depicted in Fig. 18. Generally, the models proposed by Zhao and Packer (2009) and Jamaluddin *et al.* (2013) underestimate the ultimate axial load of elliptical CFST short columns. In contrast, models proposed by Liu and Cha (2011) and Shen (2015) overestimate the ultimate axial load of elliptical CFST short columns. The model proposed by Ahmed and Liang (2020) provides fair-minded reasonable results compared with the experimental data. However, the proposed ANFIS model has superior performance in predicting the ultimate axial load of elliptical CFST short columns compared to other existing formulas. Fig. 18 shows that the R^2 values for all datasets predicted by Zhao’s formula, Liu’s formula, Jamaluddin’s formula, Shen’s formula, and Ahmed’s formula are equal to 0.856, 0.966, 0.865, 0.919, and 0.953, respectively. They are much

Table 7 Statistical results of different models

	$P_{u,exp} / P_{u,pre}$				
	Zhao and Packer (2009)	Liu and Zha (2011)	Jamaluddin <i>et al.</i> (2013)	Shen (2015)	Ahmed and Liang (2020)
Mean	1.992	0.886	2.145	0.742	1.052
<i>StD</i>	0.850	0.127	0.868	0.126	0.144
<i>CoV</i>	0.427	0.143	0.405	0.170	0.137

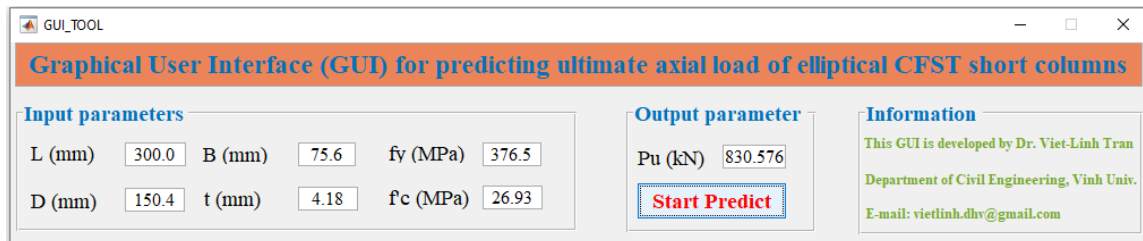


Fig. 19 Interactive GUI tool

lower than that of the proposed ANFIS model (0.986). The *RMSE* values predicted by Zhao's formula, Liu's formula, Jamaluddin's formula, Shen's formula, and Ahmed's formula are 793.60 kN, 325.258 kN, 865.357 kN, 792.169 kN, and 174.116 kN, respectively. These values show a high error compared to the proposed ANFIS model with *RMSE* value of 87.888 kN. The *a20*-index value of the proposed ANFIS model is 0.95 that is the best one compared to others. Table 7 reveals that the proposed ANFIS model achieves smallest values of the standard deviation (*StD*) and coefficient of variation (*CoV*) compared to existing formulas. The mean, *StD*, and *CoV* of test-to-prediction ultimate loads computed by Zhao's formula, Liu's formula, Jamaluddin's formula, Shen's formula, and Ahmed's formula are (1.992, 0.85, 0.427), (0.886, 0.127, 0.143), (2.145, 0.868, 0.405), (0.742, 0.126, 0.17), (1.052, 0.144, 0.137), and (1.001, 0.12, 0.102), respectively. It means that the accuracy of the proposed ANFIS model in this study is outstanding. However, it is worth noting that the confinement model proposed by Patel *et al.* (2016) yields negative lateral pressures for columns with a larger $(a + b)/t$ ratio, which may cause negative ultimate strengths. Therefore, FEM and ANFIS models in this study are only valid with the range of $(a + b)/t$ as shown in Eq. (18).

10. ANFIS-based formula and GUI tool

As indicated in the previous section, the ANFIS model can excellently predict the ultimate axial load of elliptical CFST short columns based on the current database. However, the application of the proposed ANFIS model in engineering design is not a convenient method. Thus, the proposed ANFIS model is exploited to derive an explicit formula and a GUI tool to apply for practical use. It should be noted that both explicit formula and GUI tool are derived based on the proposed ANFIS model, therefore, they provide the same results as those provided by the proposed ANFIS model. However, they are only applicable to elliptical CFST short columns with geometric and material properties within the ranges specified in Table 3. The detail of the explicit formula based

on the proposed ANFIS model and an illustrated example using this formula are described in the Appendix for practical use. Fig. 19 shows the main GUI tool, which is simple and extremely easy to use to replace the complex procedure of the explicit formula. As shown in Fig. 19, users can enter numeric values for the input parameters, then, the ultimate axial load of elliptical CFST short columns is displayed directly by clicking the Start Predict button. Obviously, the GUI tool is functional, effective and flexible. The GUI tool is provided freely at Link (Tran 2023).

11. Conclusions

In this study, an efficient ANFIS model is developed for predicting the ultimate axial load of elliptical CFST short columns. The proposed ANFIS model was trained and tested using 188 datasets and the ANFIS model with six Gaussian membership functions for each input variable and six fuzzy rules has high accuracy for determining the ultimate axial load of elliptical CFST short columns. The predictive accuracy of the proposed ANFIS model is compared with existing formulas using three performance indices (R^2 , $RMSE$ and $a20 - index$). The comparative results show that the proposed ANFIS model provides superior accuracy ($R^2=0.986$, $RMSE=87.888$, and $a20 - index=0.952$) compared to the existing formulas. In addition, an explicit formula and a GUI tool are developed to apply the proposed ANFIS model for practical use. It is clear that both explicit formula and GUI tool can be considered as the desirable and reliable methods for determining the ultimate axial load of elliptical CFST short columns. Hence, it is idealistic to have some initial estimations of the ultimate axial load of elliptical CFST short columns before performing any extensive experiment at laboratory.

References

- ACI 318 (2014), Building code requirements for structural concrete, ACI 318-14, American Concrete Institute, U.S.A.
- Ahmadi, M., Naderpour, H. and Kheyroddin, A. (2014), "Utilization of artificial neural networks to prediction of the capacity of CCFT short columns subject to short term axial load", *Arch. Civil Mech. Eng.*, **14**(3), 510-517. <https://doi.org/10.1016/j.acme.2014.01.006>
- Ahmadi, M., Naderpour, H. and Kheyroddin, A. (2017), "ANN model for predicting the compressive strength of circular steel-confined concrete", *Int. J. Civil Eng.*, **15**(2), 213-221. <https://doi.org/10.1007/s40999-016-0096-0>
- Ahmed, M., Ci, J., Yan, X. F. and Chen, S. (2021), "Nonlinear analysis of elliptical concrete-filled stainless steel tubular short columns under axial compression", *Structures*, **32**, 1374-1385. <https://doi.org/10.1016/j.istruc.2021.03.095>
- Ahmed, M. and Liang, Q.Q. (2020), "Computational simulation of elliptical concrete-filled steel tubular short columns including new confinement model", *J. Constr. Steel Res.*, **174**, 106294. <https://doi.org/10.1016/j.jcsr.2020.106294>
- ANFIS GUI tool (2023), Application of ANFIS to the design of elliptical CFST columns, Vinh University, Nghe An, Vietnam. <https://github.com/VietLinhTran/Application-of-ANFIS-to-the-design-of-elliptical-CFST-columns>
- Armaghani, D.J. and Asteris, P.G. (2021), "A comparative study of ANN and ANFIS models for the prediction of cement-based mortar materials compressive strength", *Neural Comput. Appl.*, **33**(9), 4501-4532. <https://doi.org/10.1007/s00521-020-05244-4>
- Armaghani, D.J., Hatzigeorgiou, G.D., Karamani, C., Skentou, A., Zoumpoulaki, I. and Asteris, P.G. (2019),

- “Soft computing-based techniques for concrete beams shear strength”, *Procedia Struct. Integr.*, **17**, 924-933. <https://doi.org/10.1016/j.prostr.2019.08.123>
- AS 5100.6 (2004), Bridge design-Steel and composite construction, AS 5100.6-2004, Standards Australia International Ltd GPO Box 5420, Sydney, NSW 2001, Australia.
- Asteris, P.G., Lemonis, M.E., Nguyen, T.A., Le, H.V. and Pham, B.T. (2021), “Soft computing-based estimation of ultimate axial load of rectangular concrete-filled steel tubes”, *Steel Compos. Struct.*, **39**(4), 471-491. <https://doi.org/10.12989/scs.2021.39.4.471>
- Asteris, P.G. and Mokos, V.G. (2020), “Concrete compressive strength using artificial neural networks”, *Neural Comput. Appl.*, **32**(15), 11807-11826. <https://doi.org/10.1007/s00521-019-04663-2>
- Cai, B., Pan, G. and Fu, F. (2020), “Prediction of the postfire flexural capacity of RC beam using GA-BPNN machine learning”, *J. Perform. Constr. Facilities*, **34**(6), 04020105. [https://doi.org/10.1061/\(ASCE\)CF.1943-5509.0001514](https://doi.org/10.1061/(ASCE)CF.1943-5509.0001514)
- Chan, T.M. and Gardner, L. (2008), “Compressive resistance of hot-rolled elliptical hollow sections”, *Eng. Struct.*, **30**(2), 522-532. <https://doi.org/10.1016/j.engstruct.2007.04.019>
- Chan, T.M., Gardner, L. and Law, K.H. (2010), “Structural design of elliptical hollow sections: A review”, *Proceedings of the Institution of Civil Engineers: Structures and Buildings*, **163**(6), 391-402. <https://doi.org/10.1680/stbu.2010.163.6.391>
- Chan, T.M., Huai, Y. and Wang, W. (2015), “Experimental investigation on lightweight concrete-filled cold-formed elliptical hollow section stub columns”, *J. Constr. Steel Res.*, **115**, 434-444. <https://doi.org/10.1016/j.jcsr.2015.08.029>
- Chiu, S.L. (1994), “Fuzzy model identification based on cluster estimation”, *J. Intell. Fuzzy Syst.*, **2**(3), 267-278. <https://doi.org/10.3233/IFS-1994-2306>
- Cook, R., Lapeyre, J., Ma, H. and Kumar, A. (2019), “Prediction of compressive strength of concrete: Critical comparison of performance of a hybrid machine learning model with standalone models”, *J. Mater. Civil Eng.*, **31**(11), 1-15. [https://doi.org/10.1061/\(asce\)mt.1943-5533.0002902](https://doi.org/10.1061/(asce)mt.1943-5533.0002902)
- Dai, X. and Lam, D. (2010a), “Axial compressive behaviour of stub concrete-filled columns with elliptical stainless steel hollow sections”, *Steel Compos. Struct.*, **10**(6), 517-539. <https://doi.org/10.12989/scs.2010.10.6.517>
- Dai, X. and Lam, D. (2010b), “Numerical modelling of the axial compressive behaviour of short concrete-filled elliptical steel columns”, *J. Constr. Steel Res.*, **66**(7), 931-942. <https://doi.org/10.1016/j.jcsr.2010.02.003>
- Dauji, S. (2020), “Prediction of concrete spall damage under blast: Neural approach with synthetic data”, *Comput. Concr.*, **26**(6), 533-546. <https://doi.org/10.12989/cac.2020.26.6.533>
- Ding, F.X., Yu, Z.W., Bai, Y. and Gong, Y.Z. (2011), “Elasto-plastic analysis of circular concrete-filled steel tube stub columns”, *J. Constr. Steel Res.*, **67**(10), 1567-1577. <https://doi.org/10.1016/j.jcsr.2011.04.001>
- Duan, J., Asteris, P.G., Nguyen, H., Bui, X.N. and Moayed, H. (2021), “A novel artificial intelligence technique to predict compressive strength of recycled aggregate concrete using ICA-XGBoost model”, *Eng. Comput.*, **37**(4), 3329-3346. <https://doi.org/10.1007/s00366-020-01003-0>
- Espinos, A., Gardner, L., Romero, M.L. and Hospitaler, A. (2011), “Fire behaviour of concrete filled elliptical steel columns”, *Thin Wall. Struct.*, **49**(2), 239-255. <https://doi.org/10.1016/j.tws.2010.10.008>
- Eurocode 4 (2011), Design of composite steel and concrete structures - Part 1-1: General rules and rules for buildings, **1**(2005), The European Union.
- Güneyisi, E.M., Gültekin, A. and Mermerdaş, K. (2016), “Ultimate capacity prediction of axially loaded CFST short columns”, *Int. J. Steel Struct.*, **16**(1), 99-114. <https://doi.org/10.1007/s13296-016-3009-9>
- Hassanein, M.F., Patel, V.I., El Hadidy, A.M., Al Abadi, H. and Elchalakani, M. (2018), “Structural behaviour and design of elliptical high-strength concrete-filled steel tubular short compression members”, *Eng. Struct.*, **173**, 495-511. <https://doi.org/10.1016/j.engstruct.2018.07.023>
- Ipek, S. and Güneyisi, E.M. (2019), “Ultimate axial strength of concrete-filled double skin steel tubular column sections.”, *Adv. Civil Eng.*, **2019**, 6493037. <https://doi.org/10.1155/2019/6493037>
- Jamaluddin, N., Lam, D., Dai, X. H. and Ye, J. (2013), “An experimental study on elliptical concrete filled columns under axial compression”, *J. Constr. Steel Res.*, **87**, 6-16.

- <https://doi.org/10.1016/j.jcsr.2013.04.002>
- Jang, J.R. (1993), "ANFIS: adaptive-network-based fuzzy inference system", *IEEE T. Syst. Man Cybernet.*, **23**(3), 665-685. <https://doi.org/10.1109/21.256541>
- Kar, S. and Biswal, K.C. (2020), "FRP shear contribution prediction for U-wrapped RC T-beams using a soft computing tool", *Structures*, **27**, 1093-1104. <https://doi.org/10.1016/j.istruc.2020.06.023>
- Kar, S., Pandit, A.R. and Biswal, K.C. (2020), "Prediction of FRP shear contribution for wrapped shear deficient RC beams using adaptive neuro-fuzzy inference system (ANFIS)", *Structures*, **23**, 702-717. <https://doi.org/10.1016/j.istruc.2019.10.022>
- Keshavarzi, A., Sarmadian, F., Shiri, J., Iqbal, M., Tirado-Corbalá, R. and Omran, E.S.E. (2017), "Application of ANFIS-based subtractive clustering algorithm in soil Cation Exchange Capacity estimation using soil and remotely sensed data", *Measurement*, **95**, 173-180. <https://doi.org/10.1016/j.measurement.2016.10.010>
- Lam, D., Gardner, L. and Burdett, M. (2010), "Behaviour of axially loaded concrete filled stainless steel elliptical stub columns", *Adv. Struct. Eng.*, **13**(3), 493-500. <https://doi.org/10.1260/1369-4332.13.3.493>
- Liang, Q.Q. (2009), "Performance-based analysis of concrete-filled steel tubular beam-columns, Part I: Theory and algorithms", *J. Constr. Steel Res.*, **65**(2), 363-372. <https://doi.org/10.1016/j.jcsr.2008.03.007>
- Liu, F., Wang, Y. and Chan, T.M. (2017), "Behaviour of concrete-filled cold-formed elliptical hollow sections with varying aspect ratios", *Thin Wall. Struct.*, **110**, 47-61. <https://doi.org/10.1016/j.tws.2016.10.013>
- Liu, X.C. and Zha, X.X. (2011), "Study on behavior of elliptical concrete filled steel tube members I: Stub and long columns under axial compression", *Prog. Steel Build. Struct.*, **1**, 8-14.
- Luat, N.V., Lee, J., Lee, D.H. and Lee, K. (2020), "GS-MARS method for predicting the ultimate load-carrying capacity of rectangular CFST columns under eccentric loading", *Comput. Concr.*, **25**(1), 1-14. <https://doi.org/10.12989/cac.2020.25.1.001>
- Ly, H.B., Pham, B.T., Le, L.M., Le, T.T., Le, V.M. and Asteris, P.G. (2021), "Estimation of axial load-carrying capacity of concrete-filled steel tubes using surrogate models", *Neural Comput. Appl.*, **33**(8), 3437-3458. <https://doi.org/10.1007/s00521-020-05214-w>
- Mamdani, E.H. and Assilian, S. (1975), "An experiment in linguistic synthesis with a fuzzy logic controller", *Int. J. Man Mach. Stud.*, **7**(1), 1-13. [https://doi.org/10.1016/S0020-7373\(75\)80002-2](https://doi.org/10.1016/S0020-7373(75)80002-2)
- Mander, J.B., Priestley, M.J.N. and Park, R. (1988), "Theoretical stress-strain model for confined concrete", *J. Struct. Eng.*, **114**(8), 1804-1826. [https://doi.org/10.1061/\(asce\)0733-9445\(1988\)114:8\(1804\)](https://doi.org/10.1061/(asce)0733-9445(1988)114:8(1804))
- Mirrashid, M. (2014), "Earthquake magnitude prediction by adaptive neurofuzzy inference system (ANFIS) based on fuzzy C-means algorithm", *Natural Hazards*, **74**(3), 1577-1593. <https://doi.org/10.1007/s11069-014-1264-7>
- Moon, J., Kim, J.J., Lee, T.H. and Lee, H.E. (2014), "Prediction of axial load capacity of stub circular concrete-filled steel tube using fuzzy logic", *J. Constr. Steel Res.*, **101**, 184-191. <https://doi.org/10.1016/j.jcsr.2014.05.011>
- Moon, J., Roeder, C.W., Lehman, D.E. and Lee, H.E. (2012), "Analytical modeling of bending of circular concrete-filled steel tubes", *Eng. Struct.*, **42**, 349-361. <https://doi.org/10.1016/j.engstruct.2012.04.028>
- Naderloo, L., Alimardani, R., Omid, M., Sarmadian, F., Javadikia, P., Torabi, M.Y. and Alimardani, F. (2012), "Application of ANFIS to predict crop yield based on different energy inputs", *Measure. J. Int. Measure. Confederat.*, **45**(6), 1406-1413. <https://doi.org/10.1016/j.measurement.2012.03.025>
- Nguyen, V.Q., Tran, V.L., Nguyen, D.D., Sadiq, S. and Park, D. (2022), "Novel hybrid MFO-XGBoost model for predicting the racking ratio of the rectangular tunnels subjected to seismic loading", *Transp. Geotech.*, **37**, 100878. <https://doi.org/10.1016/j.trgeo.2022.100878>
- Patel, V.I., Uy, B., Prajwal, K.A. and Aslani, F. (2016), "Confined concrete model of circular, elliptical and octagonal CFST short columns", *Steel Compos. Struct.*, **22**(3), 497-520. <https://doi.org/10.12989/scs.2016.22.3.497>
- Ren, Q., Li, M., Zhang, M., Shen, Y. and Si, W. (2019), "Prediction of ultimate axial capacity of square concrete-filled steel tubular short columns using a hybrid intelligent algorithm", *Appl. Sci.*, **9**(14). <https://doi.org/10.3390/app9142802>

- Sadrmomtazi, A., Sobhani, J. and Mirgozar, M.A. (2013), "Modeling compressive strength of EPS lightweight concrete using regression, neural network and ANFIS", *Constr. Build. Mater.*, **42**(2), 205-216. <https://doi.org/10.1016/j.conbuildmat.2013.01.016>
- Sarir, P., Chen, J., Asteris, P.G., Armaghani, D.J. and Tahir, M.M. (2021), "Developing GEP tree-based, neuro-swarm, and whale optimization models for evaluation of bearing capacity of concrete-filled steel tube columns", *Eng. Comput.*, **37**(1), 1-19. <https://doi.org/10.1007/s00366-019-00808-y>
- Shariati, M., Mafipour, M.S., Haido, J.H., Yousif, S.T., Toghroli, A., Trung, N.T. and Shariati, A. (2020), "Identification of the most influencing parameters on the properties of corroded concrete beams using an Adaptive Neuro-Fuzzy Inference System (ANFIS)", *Comput. Concr.*, **25**(1), 155-170. <https://doi.org/10.12989/cac.2020.25.1.083>
- Sheehan, T., Dai, X.H., Chan, T.M. and Lam, D. (2012), "Structural response of concrete-filled elliptical steel hollow sections under eccentric compression", *Eng. Struct.*, **45**, 314-323. <https://doi.org/10.1016/j.engstruct.2012.06.040>
- Shen, Q., Wang, J., Wang, W. and Wang, J. (2015), "Axial compressive behavior and bearing capacity calculation of ECFST columns based on numerical analysis", *Prog. Steel Build. Struct.*, **17**(6), 68-78. <https://doi.org/10.13969/j.cnki.cn31-1893.2015.06.009>
- Sklar, S., Fish, D. and Simpson Stern, C. (2017), "Reflections", *Text Perform. Quarter.*, **37**(2), 169-170. <https://doi.org/10.1080/10462937.2017.1349256>
- Sugeno, M. (1985), "An introductory survey of fuzzy control", *Inform. Sci.*, **36**(1-2), 59-83. [https://doi.org/10.1016/0020-0255\(85\)90026-X](https://doi.org/10.1016/0020-0255(85)90026-X)
- Sun, G., Hasanipanah, M., Bakhshandeh Amnieh, H. and Foong, L.K. (2020), "Feasibility of indirect measurement of bearing capacity of driven piles based on a computational intelligence technique", *Measure. J. Int. Measure. Confederat.*, **156**, 107577. <https://doi.org/10.1016/j.measurement.2020.107577>
- Systèmes, D. (2014), Abaqus version 6.14-4 documentation. Waltham, MA: Dassault Systems Simulia Corporation.
- Tran, V.L., Ahmed, M. and Gohari, S. (2023), "Prediction of the ultimate axial load of circular concrete-filled stainless steel tubular columns using machine learning approaches", *Struct. Concr.*, 2023. <https://doi.org/10.1002/suco.202200877>
- Tran, V.L. and Kim, J.K. (2023a), "Innovative formulas for reinforcing bar bonding failure stress of tension lap splice using ANN and TLBO", *Constr. Build. Mater.*, **369**, 130500. <https://doi.org/10.1016/j.conbuildmat.2023.130500>
- Tran, V.L. and Kim, J.K. (2023b), "Ensemble machine learning-based models for estimating the transfer length of strands in PSC beams", *Exp. Syst. Appl.*, **221**, 119768. <https://doi.org/10.1016/j.eswa.2023.119768>
- Tran, V.L. and Kim, S.E. (2020), "Efficiency of three advanced data-driven models for predicting axial compression capacity of CFST columns", *Thin Wall. Struct.*, **152**, 106744. <https://doi.org/10.1016/j.tws.2020.106744>
- Tran, V.L., Thai, D.K. and Kim, S.E. (2019a), "Application of ANN in predicting ACC of SCFST column", *Compos. Struct.*, **228**. <https://doi.org/10.1016/j.compstruct.2019.111332>
- Tran, V.L., Thai, D.K. and Kim, S.E. (2019b), "A new empirical formula for prediction of the axial compression capacity of CCFT columns", *Steel Compos. Struct.*, **33**(2), 181-194. <https://doi.org/10.12989/scs.2019.33.2.181>
- Uenaka, K. (2014), "Experimental study on concrete filled elliptical/oval steel tubular stub columns under compression", *Thin Wall. Struct.*, **78**, 131-137. <https://doi.org/10.1016/j.tws.2014.01.023>
- Umrao, R.K., Sharma, L.K., Singh, R. and Singh, T.N. (2018), "Determination of strength and modulus of elasticity of heterogenous sedimentary rocks: An ANFIS predictive technique", *Measure. J. Int. Measure. Confederat.*, **126**, 194-201. <https://doi.org/10.1016/j.measurement.2018.05.064>
- Vahidi, E.K., Malekabi, M.M., Rezaei, A., Roshani, M.M. and Roshani, G.H. (2017), "Modeling of mechanical properties of roller compacted concrete containing RHA using ANFIS", *Comput. Concr.*, **19**(4), 435-442. <https://doi.org/10.12989/cac.2017.19.4.435>
- Vakhshouri, B. and Nejadi, S. (2018), "Prediction of compressive strength of self-compacting concrete by

- ANFIS models”, *Neurocomputing*, **280**, 13-22. <https://doi.org/10.1016/j.neucom.2017.09.099>
- Xue, X. and Zhou, H. (2018), “Neuro-fuzzy based approach for estimation of concrete compressive strength”, *Comput. Concr.*, **21**(6), 697-703. <https://doi.org/10.12989/cac.2018.21.6.697>
- Yang, H., Lam, D. and Gardner, L. (2008), “Testing and analysis of concrete-filled elliptical hollow sections”, *Eng. Struct.*, **30**(12), 3771-3781. <https://doi.org/10.1016/j.engstruct.2008.07.004>
- Yang, H., Liu, F., Chan, T. and Wang, W. (2017), “Behaviours of concrete-filled cold-formed elliptical hollow section beam-columns with varying aspect ratios”, *Thin Wall. Struct.*, **120**, 9-28. <https://doi.org/10.1016/j.tws.2017.08.018>
- Yaylacı, E.U., Yaylacı, M., Ölmez, H. and Birinci, A. (2020), “Artificial neural network calculations for a receding contact problem”, *Comput. Concr.*, **25**(6), 551-563. <https://doi.org/10.12989/cac.2020.25.6.551>
- Zha, X., Gong, G. and Liu, X. (2013), “Study on behavior of concrete filled elliptical steel tube members part I: Short and long columns under axial compression”, *Group Org. Manag.*, **38**(4), 90-107. http://en.cnki.com.cn/Article_en/CJFDTotal-JZJZ201101005.htm
- Zhao, X.L. and Packer, J.A. (2009), “Tests and design of concrete-filled elliptical hollow section stub columns”, *Thin Wall. Struct.*, **47**(6-7), 617-628. <https://doi.org/10.1016/j.tws.2008.11.004>
- Zorlu, K., Gokceoglu, C., Ocakoglu, F., Nefeslioglu, H.A. and Acikalin, S. (2008), “Prediction of uniaxial compressive strength of sandstones using petrography-based models”, *Eng. Geol.*, **96**(3-4), 141-158. <https://doi.org/10.1016/j.enggeo.2007.10.009>

CC

Nomenclature

CFST	Concrete-filled steel tubular	η_c	Effect of confinement in the concrete strength
ANFIS	Adaptive neuro-fuzzy inference system	EI	Flexural rigidity of the elliptical cross-section
GUI	Graphical user interface	λ	Slenderness ratio
P	Axial compression load	E_s	Elastic modulus of the steel tubular
L	Length of the column	I_s	Inertia moment of the steel tubular
D	Major axis diameter	E_c	Elastic modulus of the core concrete
B	Minor axis diameter	I_c	Inertia moment of the core concrete
t	Thickness of the steel tubular	μ	Effective length factor
FE	Finite element	f_{sc}	Unified strength
ML	Machine learning	f_{ck}	Axial compressive strength of unconfined concrete
ANN	Artificial neural network	ξ	Factor of confinement effect

A_s	Cross-sectional area of steel tubular	f_{cu}	Compressive strength of cubic specimen concrete core
A_c	Cross-sectional area of concrete	MF	Membership function
f_y	Yield strength of the steel tubular	FIS	Fuzzy inference system
f'_c	Compressive strength of the concrete core	StD	Standard deviation
D_e	Equivalent diameter of elliptical section	CoV	Coefficient of variation
a	A half of the major axis diameter	R^2	Coefficient of determination
b	A half of the minor axis diameter	$RMSE$	Root mean squared error
η_s	A factor to reduce the steel tubular strength to account for hoop stress	$a20$ – index	Ratio of the predicted value to a target value falling between 0.80 and 1.20

Appendix. Explicit formula based on the proposed ANFIS

The ultimate axial load of elliptical CFST short columns in kN is expressed as

$$P_u = 2944.99P_{uN} + 389.1, \text{ kN} \quad (31)$$

where P_{uN} and P_u are the normalized and actual predicted value of the ultimate axial load, respectively.

The normalized value of the ultimate axial load can be determined by

$$P_{uN} = \frac{\sum_{i=1}^6 W_i CL_i}{\sum_{i=1}^6 W_i} \quad (32)$$

where W_i are the rule's weights for each rule, CL_i are clusters.

The clusters are expressed as

$$\begin{aligned}
 CL_1 &= -0.205X_1^N + 0.635X_2^N + 0.156X_3^N + 0.598X_4^N + 0.113X_5^N + 0.224X_6^N - 0.199 \\
 CL_2 &= -0.338X_1^N + 0.727X_2^N + 0.361X_3^N + 0.547X_4^N + 0.163X_5^N + 0.169X_6^N - 0.345 \\
 CL_3 &= -0.201X_1^N + 0.743X_2^N + 0.409X_3^N + 0.446X_4^N + 0.209X_5^N + 0.159X_6^N - 0.329 \\
 CL_4 &= -0.296X_1^N + 0.741X_2^N + 0.368X_3^N + 0.493X_4^N + 0.199X_5^N + 0.188X_6^N - 0.322 \\
 CL_5 &= -0.359X_1^N + 0.662X_2^N + 0.275X_3^N + 0.602X_4^N + 0.124X_5^N + 0.175X_6^N - 0.437 \\
 CL_6 &= -0.277X_1^N + 0.669X_2^N + 0.298X_3^N + 0.715X_4^N + 0.207X_5^N + 0.238X_6^N - 0.298
 \end{aligned} \quad (33)$$

where $X_i^N, i = 1 - 6$ are the normalized values of input variables, which are expressed in Eq. (28).

From MFs presented in Table 5, the rule's weight parameters, W_i ($i = 1, \dots, 6$) are calculated as

$$\begin{aligned}
 W_1 &= \left(e^{\frac{-(X_1^N - 0.097)^2}{0.032}} \right) \left(e^{\frac{-(X_2^N - 0.296)^2}{0.014}} \right) \left(e^{\frac{-(X_3^N - 0.223)^2}{0.005}} \right) \left(e^{\frac{-(X_4^N - 0.087)^2}{0.033}} \right) \left(e^{\frac{-(X_5^N - 0.183)^2}{0.051}} \right) \left(e^{\frac{-(X_6^N - 0.047)^2}{0.086}} \right) \\
 W_2 &= \left(e^{\frac{-(X_1^N - 0.491)^2}{0.015}} \right) \left(e^{\frac{-(X_2^N - 0.525)^2}{0.013}} \right) \left(e^{\frac{-(X_3^N - 0.085)^2}{0.028}} \right) \left(e^{\frac{-(X_4^N - 0.673)^2}{0.011}} \right) \left(e^{\frac{-(X_5^N - 0.451)^2}{0.006}} \right) \left(e^{\frac{-(X_6^N - 0.708)^2}{0.063}} \right) \\
 W_3 &= \left(e^{\frac{-(X_1^N - 0.286)^2}{0.016}} \right) \left(e^{\frac{-(X_2^N - 0.302)^2}{0.007}} \right) \left(e^{\frac{-(X_3^N - 0.210)^2}{0.006}} \right) \left(e^{\frac{-(X_4^N - 0.448)^2}{0.023}} \right) \left(e^{\frac{-(X_5^N - 0.444)^2}{0.010}} \right) \left(e^{\frac{-(X_6^N - 0.791)^2}{0.046}} \right)
 \end{aligned} \tag{34}$$

$$W_4 = \left(e^{\frac{-(X_1^N - 0.265)^2}{0.005}} \right) \left(e^{\frac{-(X_2^N - 0.302)^2}{0.002}} \right) \left(e^{\frac{-(X_3^N - 0.213)^2}{0.023}} \right) \left(e^{\frac{-(X_4^N - 0.375)^2}{0.034}} \right) \left(e^{\frac{-(X_5^N - 0.494)^2}{0.016}} \right) \left(e^{\frac{-(X_6^N - 0.237)^2}{0.054}} \right)$$

$$W_5 = \left(e^{\frac{-(X_1^N - 0.363)^2}{0.009}} \right) \left(e^{\frac{-(X_2^N - 0.385)^2}{0.011}} \right) \left(e^{\frac{-(X_3^N - 0.322)^2}{0.019}} \right) \left(e^{\frac{-(X_4^N - 0.529)^2}{0.009}} \right) \left(e^{\frac{-(X_5^N - 0.447)^2}{0.001}} \right) \left(e^{\frac{-(X_6^N - 0.637)^2}{0.026}} \right)$$

$$W_6 = \left(e^{\frac{-(X_1^N - 0.503)^2}{0.018}} \right) \left(e^{\frac{-(X_2^N - 0.551)^2}{0.013}} \right) \left(e^{\frac{-(X_3^N - 0.516)^2}{0.014}} \right) \left(e^{\frac{-(X_4^N - 0.663)^2}{0.010}} \right) \left(e^{\frac{-(X_5^N - 0.499)^2}{0.012}} \right) \left(e^{\frac{-(X_6^N - 0.803)^2}{0.066}} \right)$$

where X_1^N , X_2^N , X_3^N , X_4^N , X_5^N and X_6^N are the normalized values of the input variables.